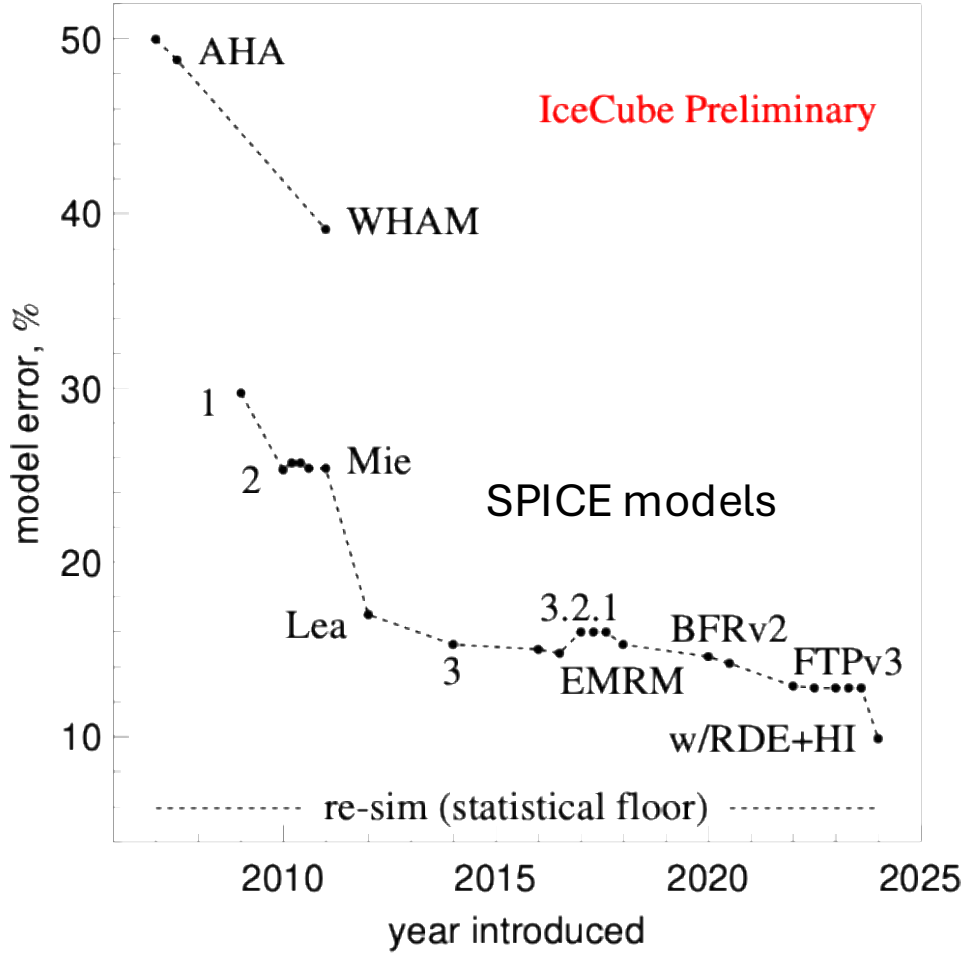
State of the Ice Model in the IceCube Observatory



AMANDA-A (1994): dominated by air bubbles

AMANDA II (2006): clear ice at depths 1.4-2.3 km

IceCube (2009): direct fit to simulation

IceCube (2013): layer tilt, ice anisotropy

IceCube (2023): birefringence, precise 2d tilt

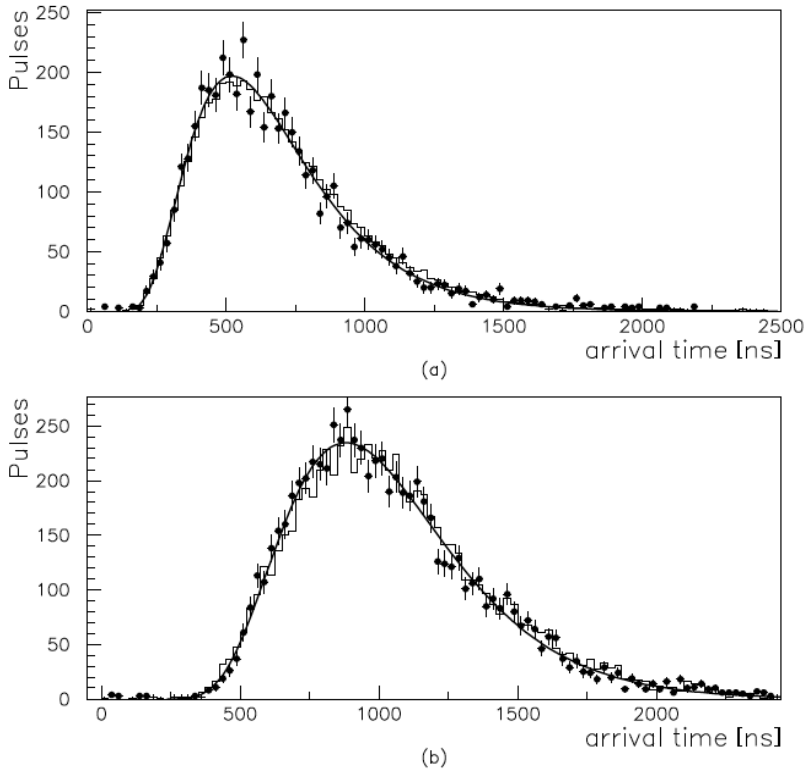
Goodness of fit, model error, statistical floor

Ice calibration plans with IceCube Upgrade

Albrecht Karle for the IceCube Collaboration

NSF | IceCube Neutrino Observatory | WIPAC Wisconsin IceCube Particle Astrophysics Center | FAU | ecap Erlangen Centre for Astroparticle Physics

AMANDA-A: scattering on air bubbles!



$$u(d,t) = \frac{1}{(4\pi Dt)^{3/2}} e^{\frac{-d^2}{4Dt}} e^{\frac{-c_i t}{\lambda_a}}$$

Analytical description (diffusive regime)
Possible due to very small scattering length

1994

astro-ph/9412028 08 Dec 1994

Optical Properties of the South Pole Ice
at Depths Between 0.8 and 1 km

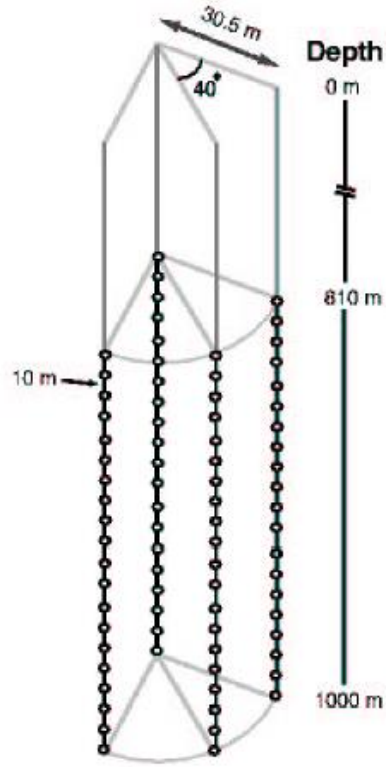
P. Askebjer, S.W. Barwick, L. Bergström, A. Bouchta, S. Carius, A. Coulthard, K. Engel, B. Erlandsson, A. Goobar, L. Gray, A. Hallgren, F. Halzen, P.O. Hulth, J. Jacobsen, S. Johansson, V. Kandhadai, I. Liubarsky, D. Lowder, T. Miller, P.C. Mock, R. Morse, R. Porrata, P.B. Price, A. Richards, H. Rubinstein, E. Schneider, Q. Sun, S. Tilav, C. Walck & G. Yodh

The optical properties of the ice at the geographical South Pole have been investigated at depths between 0.8 and 1 kilometers. The absorption and scattering lengths of visible light (~515 nm) have been measured *in situ* using the laser calibration setup of the AMANDA neutrino detector. The ice is intrinsically extremely transparent. The measured absorption length is 59 ± 3 meters, comparable with the quality of the ultra-

Distance between sensors 10 m
Long absorption length: 60-200 m
Short effective scattering length: 1 m

→ Very clean ice with low impurities
→ Scattering due to air bubbles

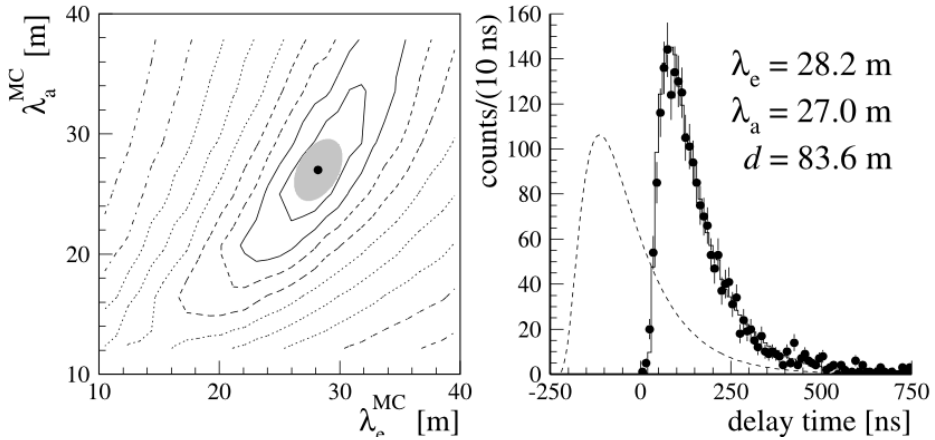
Air bubbles predicted to disappear
(convert to clathrate hydrates) at 1150 m

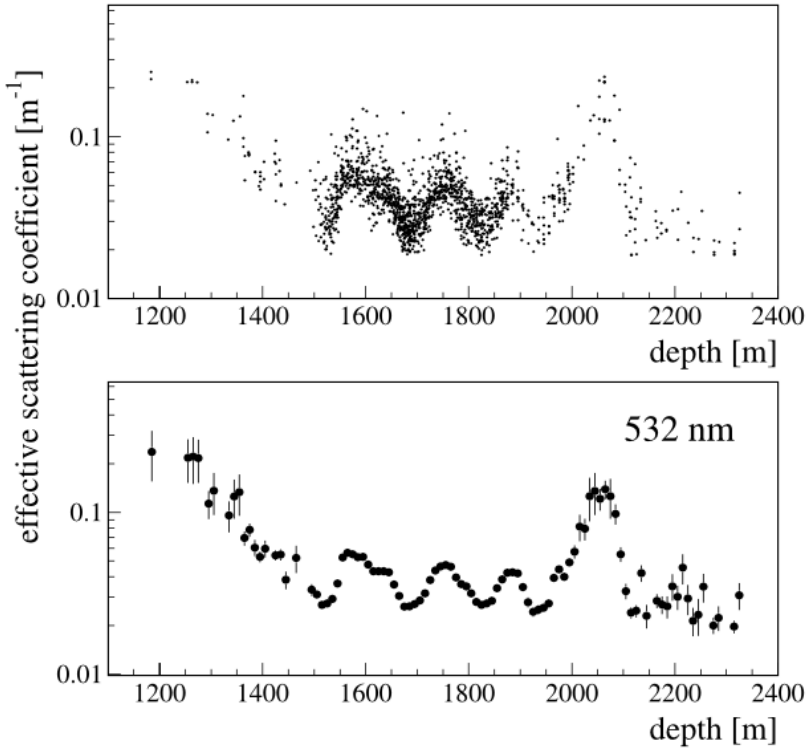


$$\lambda_a = 59 \pm 1 \text{ m, and}$$

$$\frac{1}{\lambda_{bub}} = \frac{(28.6 \pm 1.1) - (0.025 \pm 0.001)z}{4(1-\tau)} \; m^{-1}$$

AMANDA-II: comprehensive ice model





JOURNAL OF GEOPHYSICAL RESEARCH, VOL. 111, D13203, doi:10.1029/2005JD006687, 2006

2006

Optical properties of deep glacial ice at the South Pole

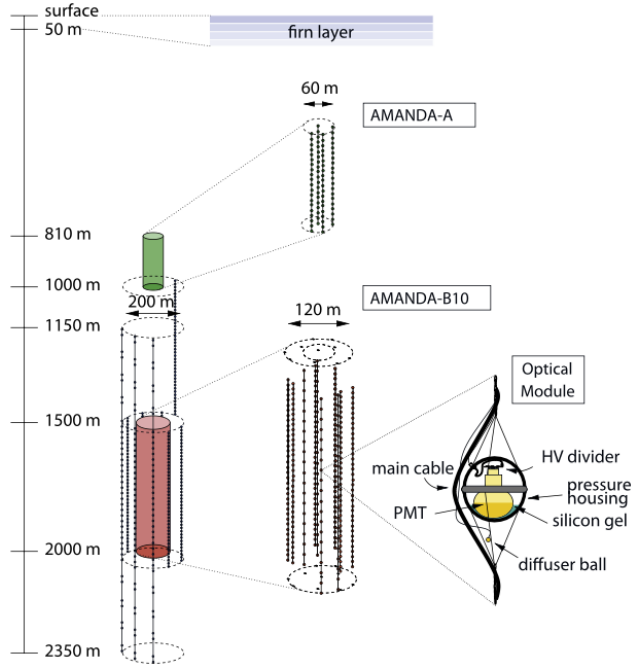
M. Ackermann,[1] J. Ahrens,[2] X. Bai,[3] M. Bartelt,[4] S. W. Barwick,[5] R. C. Bay,[6] T. Becka,[2] J. K. Becker,[4] K.-H. Becker,[7] P. Berghaus,[8] E. Bernardini,[1] D. Bertrand,[8] D. J. Boersma,[9] S. Böser,[1] O. Botner,[10] A. Bouchta,[10] O. Bouhali,[8] C. Burgess,[11] T. Burgess,[11] T. Castermans,[12] D. Chirkin,[13] B. Collin,[14] J. Conrad,[10] J. Cooley,[9] D. F. Cowen,[14] A. Davour,[10] C. De Clercq,[15] C. P. de los Heros,[10] P. Desiati,[9] T. DeYoung,[14] P. Ekström,[11] T. Feser,[2] T. K. Gaisser,[3] R. Ganugapati,[9] H. Geenen,[7] L. Gerhardt,[5] A. Goldschmidt,[13] A. Groß,[4] A. Hallgren,[10] F. Halzen,[9] K. Hanson,[9] D. H. Hardtke,[6] T. Harenberg,[7] T. Hauschildt,[3] K. Helbing,[13] M. Hellwig,[2] P. Herquet,[12] G. C. Hill,[9] J. Hodges,[9] D. Hubert,[15] B. Hughey,[9] P. O. Hulth,[11] K. Hultqvist,[11] S. Hundertmark,[11] J. Jacobsen,[13]

Found clean ice at detector depths

Confirmed absence of air bubbles, refined their disappearance depth to 1350 m

Fitted λ_a and λ_e to each emitter-receiver pair, had to average for each 10 m ice layer

Limitation of this method, later understood: average values did not describe well fitted emitter-receiver pairs. Need to fit entire ice depth table simultaneously from the start.



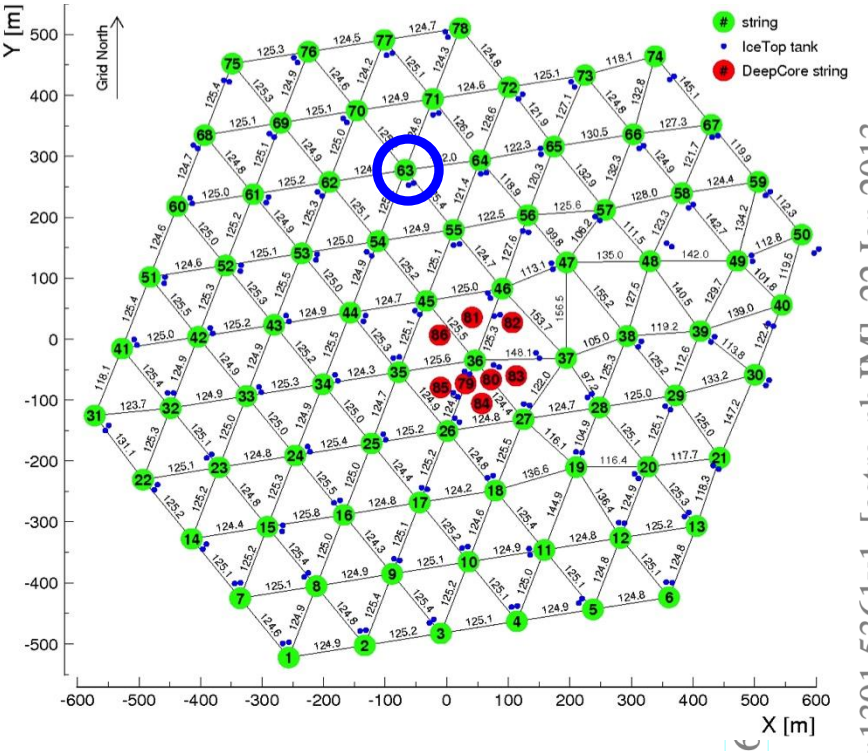
Ice cleaner than best lab ice

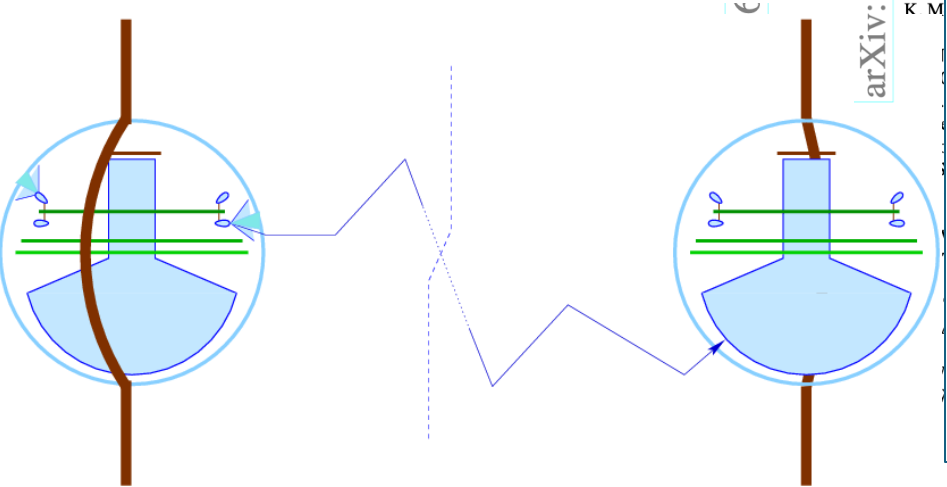
Concept of 10 m layered ice

Wavelength dependence

Air bubble fit

SPICE models: simultaneous direct fit to all layers



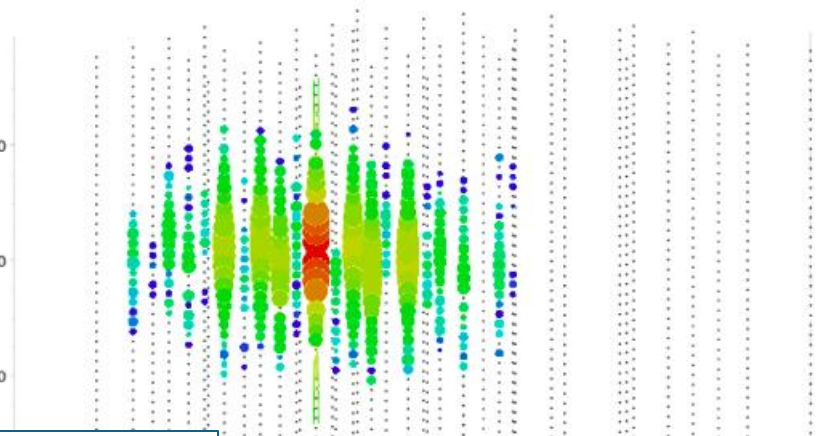


arXiv:1301.5361v1 [astro-ph.IM] 22 Jan 2013

Measurement of South Pole ice transparency with the IceCube LED calibration system

2013

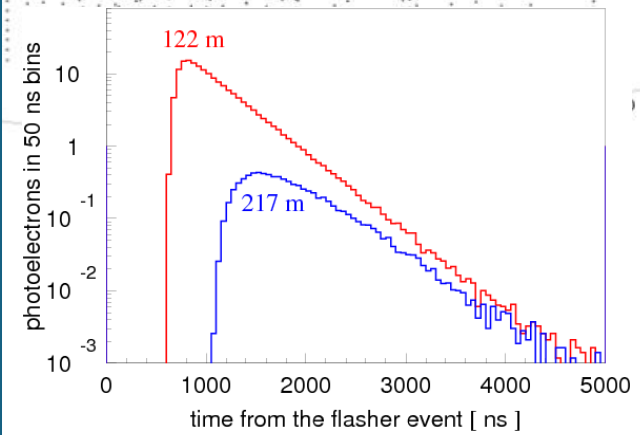
M. G. Aartsen[b], R. Abbasi[aa], Y. Abdou[v], M. Ackermann[ao], J. Adams[o], J. A. Aguilar[u], M. Ahlers[aa], D. Altmann[i], J. Auffenberg[aa], X. Bai[ae,l], M. Baker[aa], S. W. Barwick[w], V. Baum[ab], R. Bay[g], J. J. Beatty[q,r], S. Bechet[l], J. Becker Tjus[j], K.-H. Becker[an], M. Bell[al], M. L. Benabderrahmane[ao], S. BenZvi[aa], J. Berdermann[ao], P. Berghaus[ao], D. Berley[p], E. Bernardini[ao], A. Bernhard[ad], D. Bertrand[l], D. Z. Besson[y], G. Binder[h,g], D. Bindig[an], M. Bissok[a], E. Blaufuss[p], J. Blumenthal[a], D. J. Boersma[am], S. Bohaichuk[t], C. Bohm[ah], D. Bose[m], S. Böser[k], O. Botner[am], L. Brayeur[m], A. M. Brown[o], R. Bruijn[x], J. Brunner[ao], S. Buitink[m], M. Carson[v], J. Casey[e], M. Casier[m], D. Chirkin[aa,5,*], B. Christy[p], K. Clark[al], F. Clevermann[s], S. Cohen[x], D. F. Cowen[al,ak], A. H. Cruz Silva[ao], M. Danninger[ah], J. Daughhetee[e], J. C. Davis[q], C. De Clercq[m], S. De Ridder[v], P. Desiati[aa], M. de With[i], T. DeYoung[al], J. C. Díaz-Vélez[aa], M. Dunkman[al], R. Eagan[al], B. Eberhardt[ab], J. Eisch[aa],



Fitted the entire λ_a, λ_e ice depth table to all calibration data simultaneously → this overcomes previous limitation in 2006 paper

Developed photon propagation code (ppc), which re-simulates calibration data on the spot, allows for easy updates to simulation when tweaking the underlying ice model

In later sets, 12 LEDs on each of nearly 5160 DOMs are flashed individually, with 100s of receivers for each event with many time bins for each → a wealth of data



Ice layer tilt

Ice at the South Pole is flowing downhill at a rate of ~10 m/year

While the surface of the ice is flat, the bottom of the ice sheet rests atop of bedrock, which has irregular features such as hills and valleys

The ice sheet deforms as it flows through these features, and this results in lower ice layers following the shape of the bedrock; the closer to bedrock, the more the ice layers deviate from the flat that we see on the surface

An ice layer consists of ice deposited at around the same time, so should have the same concentration of impurities across the layer, thus same scattering and absorption properties. The "dirtier" layers will create bands of reflected radar signal

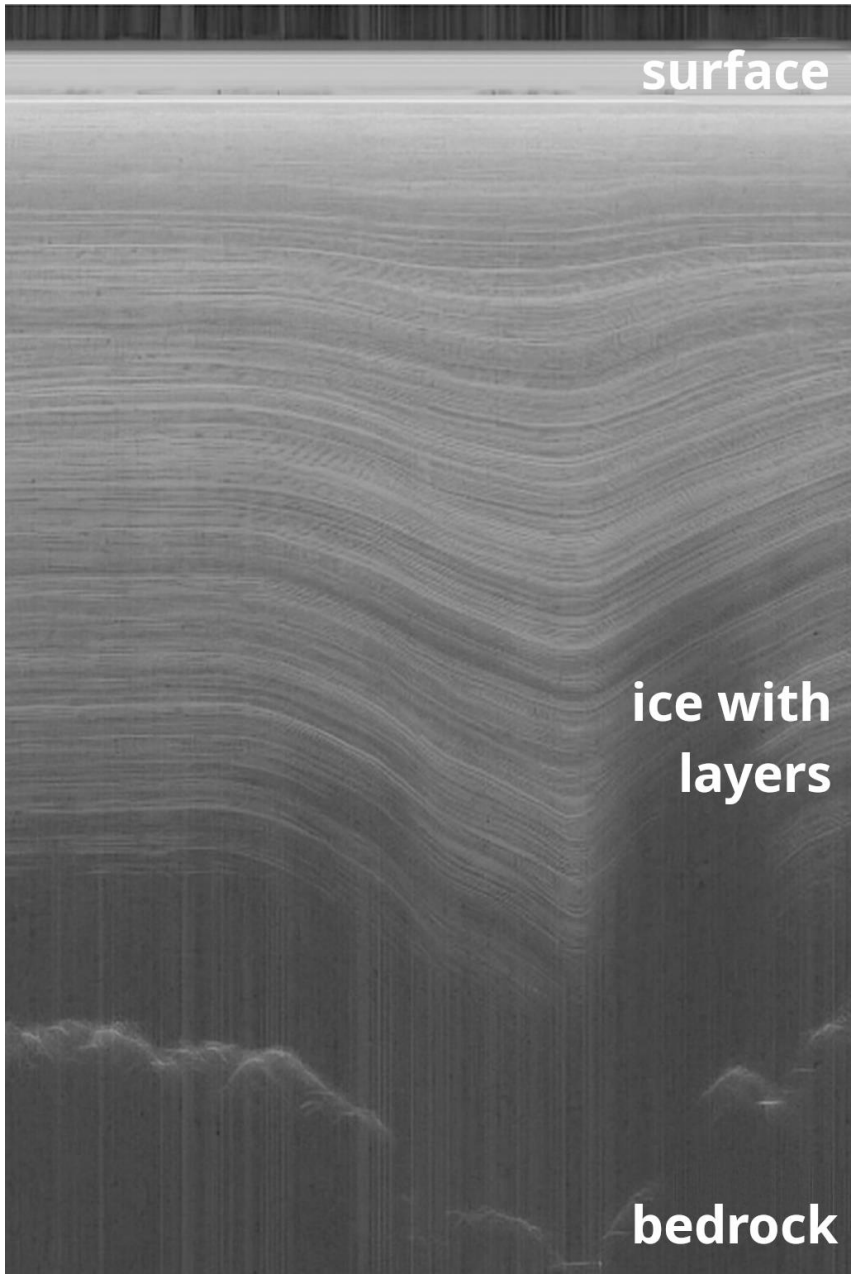


Illustration borrowed from RAID

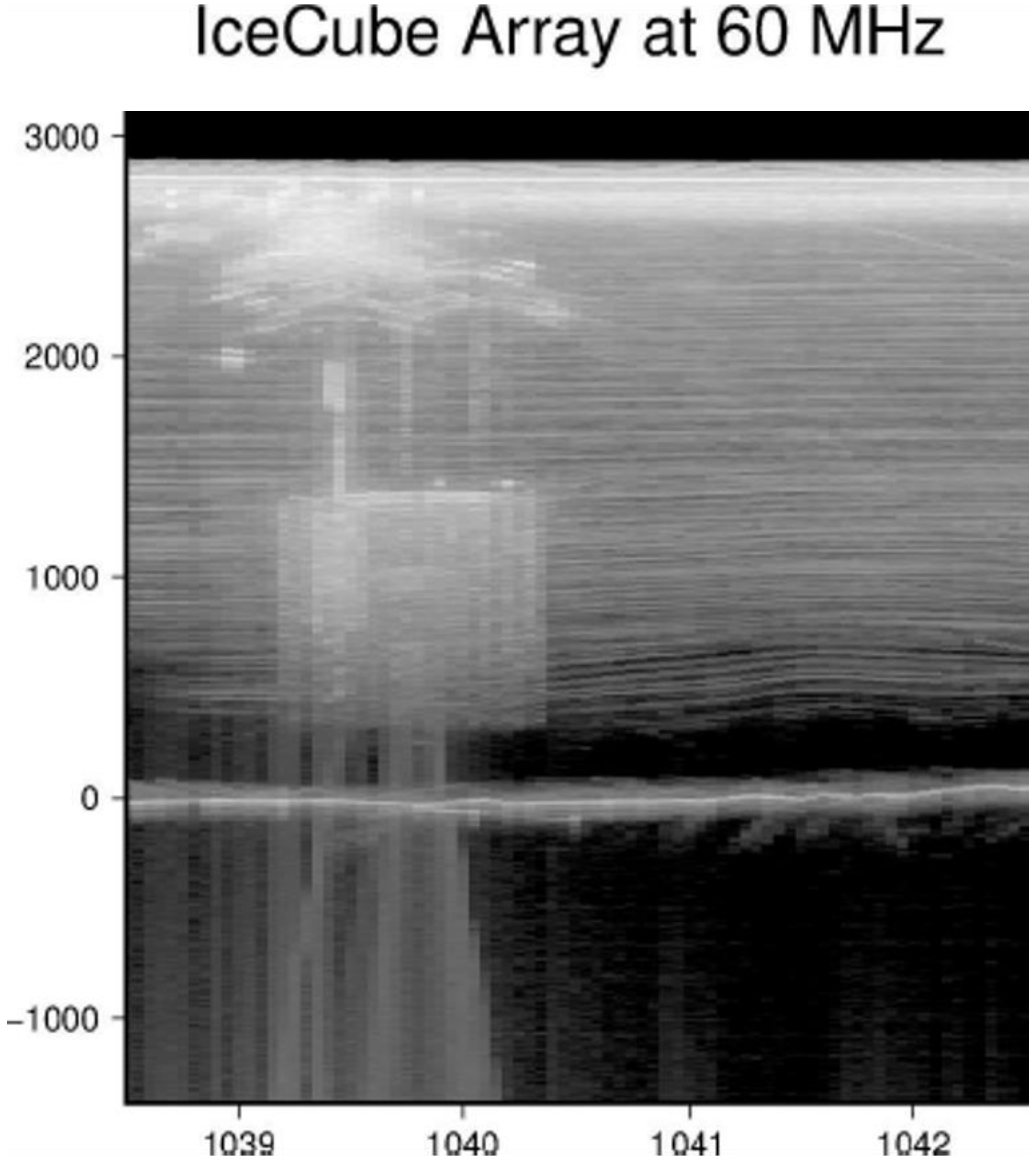
Ice layer tilt

Ice at the South Pole is flowing downhill at a rate of ~10 m/year

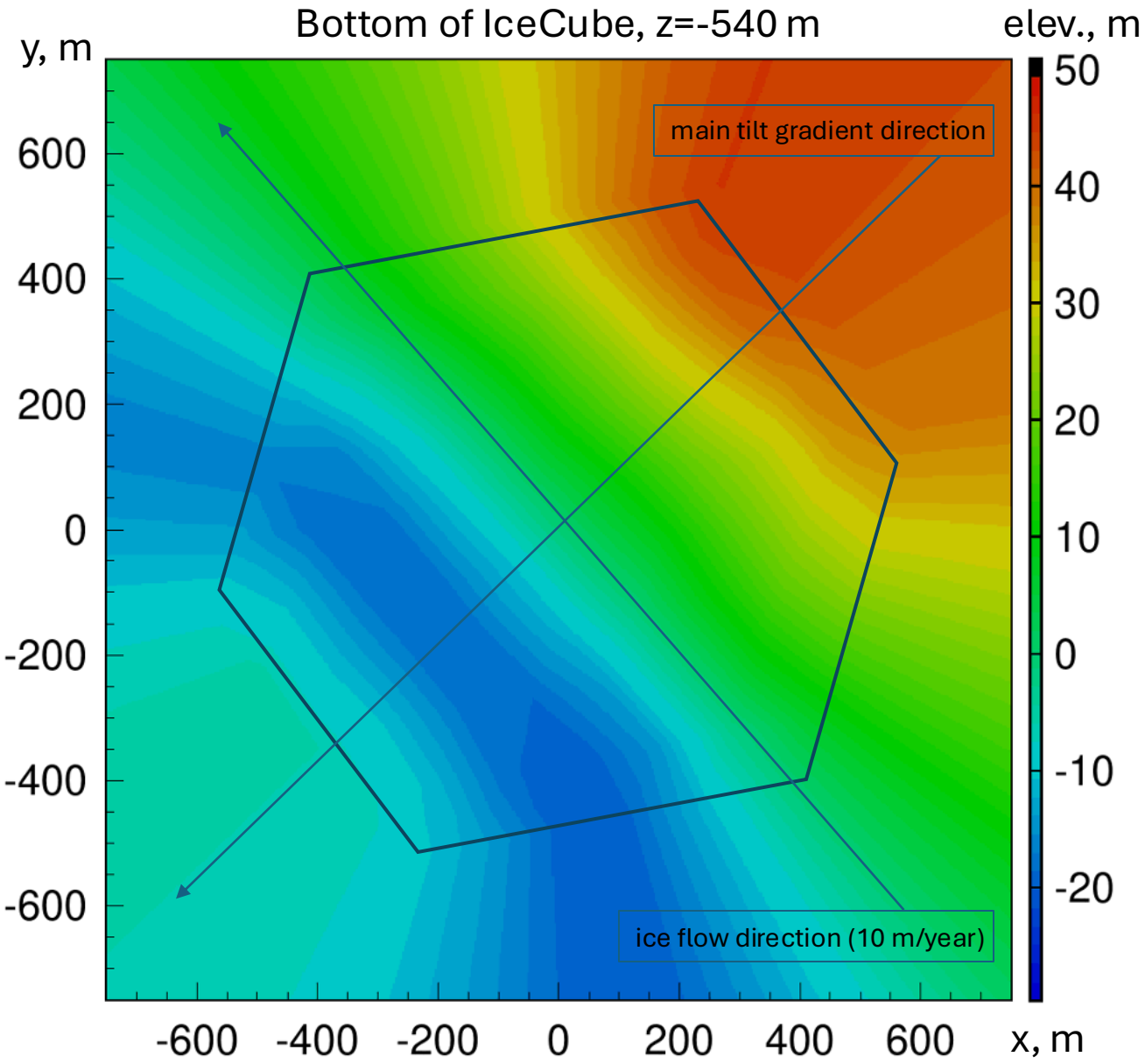
While the surface of the ice is flat, the bottom of the ice sheet rests atop of bedrock, which has irregular features such as hills and valleys

The ice sheet deforms as it flows through these features, and this results in lower ice layers following the shape of the bedrock; the closer to bedrock, the more the ice layers deviate from the flat that we see on the surface

An ice layer consists of ice deposited at around the same time, so should have the same concentration of impurities across the layer, thus same scattering and absorption properties. The “dirtier” layers will create bands of reflected radar signal



Ice tilt fitted with IceCube calibration data



Ice layer elevations relative to a point near center are tabulated on a hexagonal grid of 80 xy points, 125 depth values per xy point.

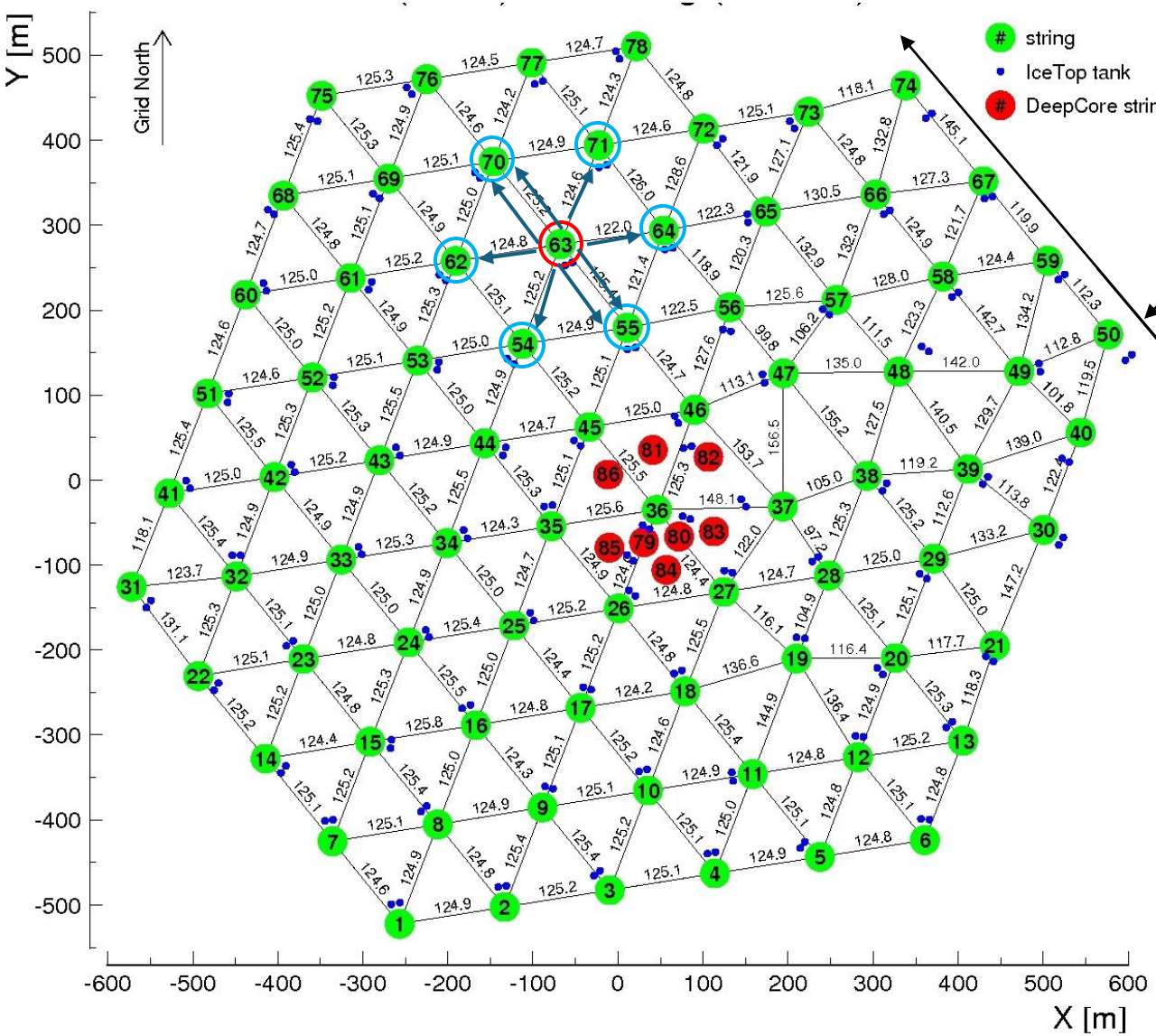
Regions outside of detector hexagon outline, above and below +-500 m are extrapolations

The 1d gradient tilt (only accounting for tilt in the direction NE-SW) appears to be a better approximation at the bottom of the detector

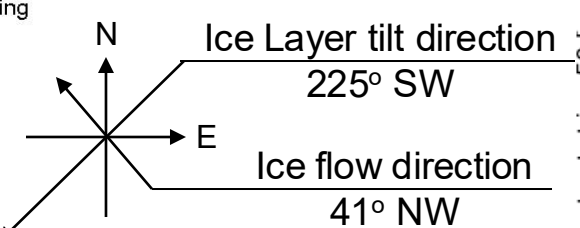
Across the entire fitted depth range there appears to be an additional component that changes the depth of ice layers along the ice flow (layers getting shallower downstream)

Nearly 2 years of fitting to ~10k parameters and a correlation matrix. Regularizations, sparsity conditions, were needed.

Glacial ice flow, ice layer tilt, and optical anisotropy



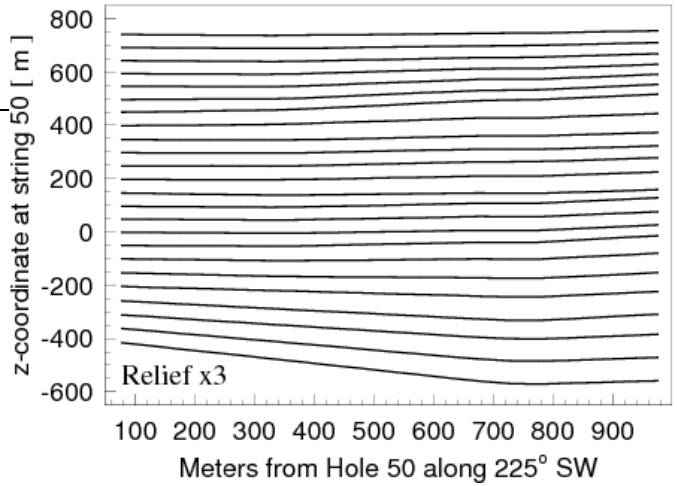
SPICE Lea

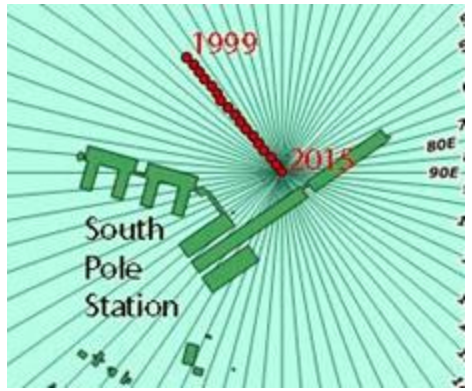


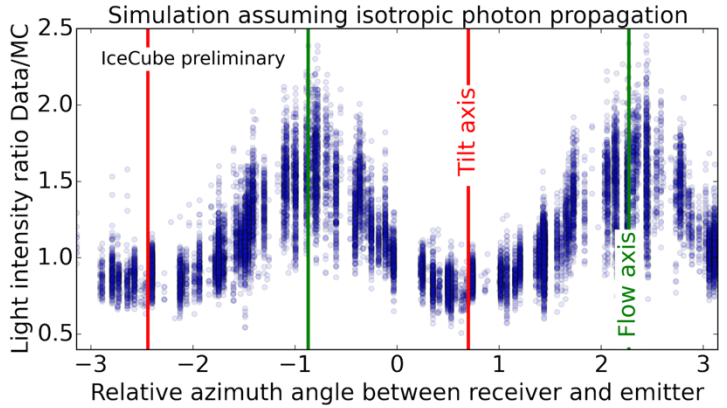
Ice Layer tilt direction
225° SW

Ice flow direction
41° NW

Less attenuation
41° NW

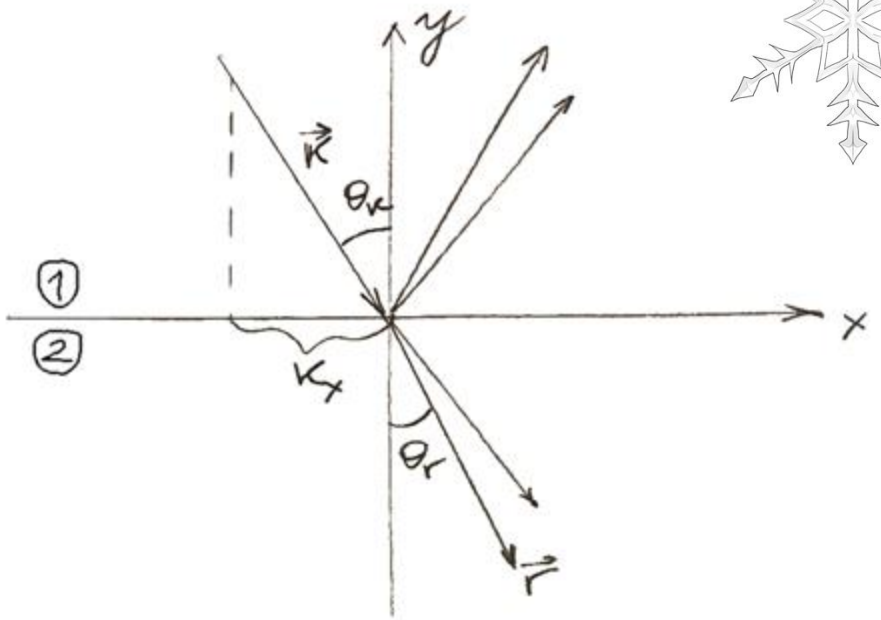






Optical anisotropy of ice due to Birefringence

- Ice is a uniaxial birefringent material with n_e-n_o=0.0015. This tiny difference builds to a macroscopic effect due to 1000s of ice crystal boundaries crossed per meter of distance
- At each grain boundary every ray is split into two reflected and two refracted rays, one ordinary and one extraordinary ray each, building to a diffusion pattern after a few scatters
- Each ice crystal has a hexagonal lattice structure, easiest to deform along the basal (hexagon) plane
- Forces associated with the ice flow, and hydrostatic pressure at depth, result in preferred ice crystal orientations at depth, in particular “girdle” fabric of ice crystal optical axis orientations around the ice flow
- This builds into 2 macroscopic effects: larger diffusion along, and slow bending of the photon path towards the ice flow



$$\begin{aligned}
\hat{n} \cdot \boldsymbol{D}_2 &= \hat{n} \cdot \boldsymbol{D}_1 \\
\hat{n} \cdot \boldsymbol{B}_2 &= \hat{n} \cdot \boldsymbol{B}_1 \\
\hat{n} \times \boldsymbol{E}_2 &= \hat{n} \times \boldsymbol{E}_1 \\
\hat{n} \times \boldsymbol{H}_2 &= \hat{n} \times \boldsymbol{H}_1.
\end{aligned}$$

Hence we can make the following observations:

1. Normal components of $\boldsymbol{D}$ and $\boldsymbol{B}$ are continuous across a dielectric interface
2. Tangential components of $\boldsymbol{E}$, $\boldsymbol{H}$ are continuous across a dielectric surface

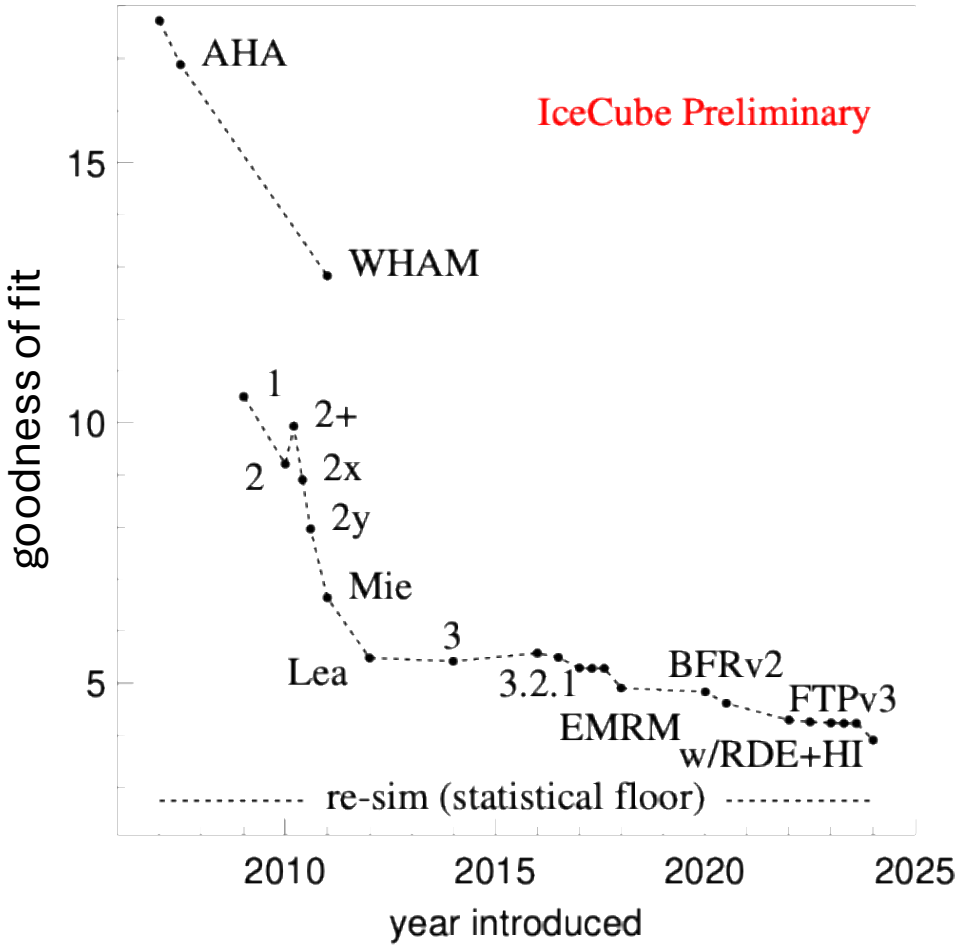
SPICE model vs. statistical floor

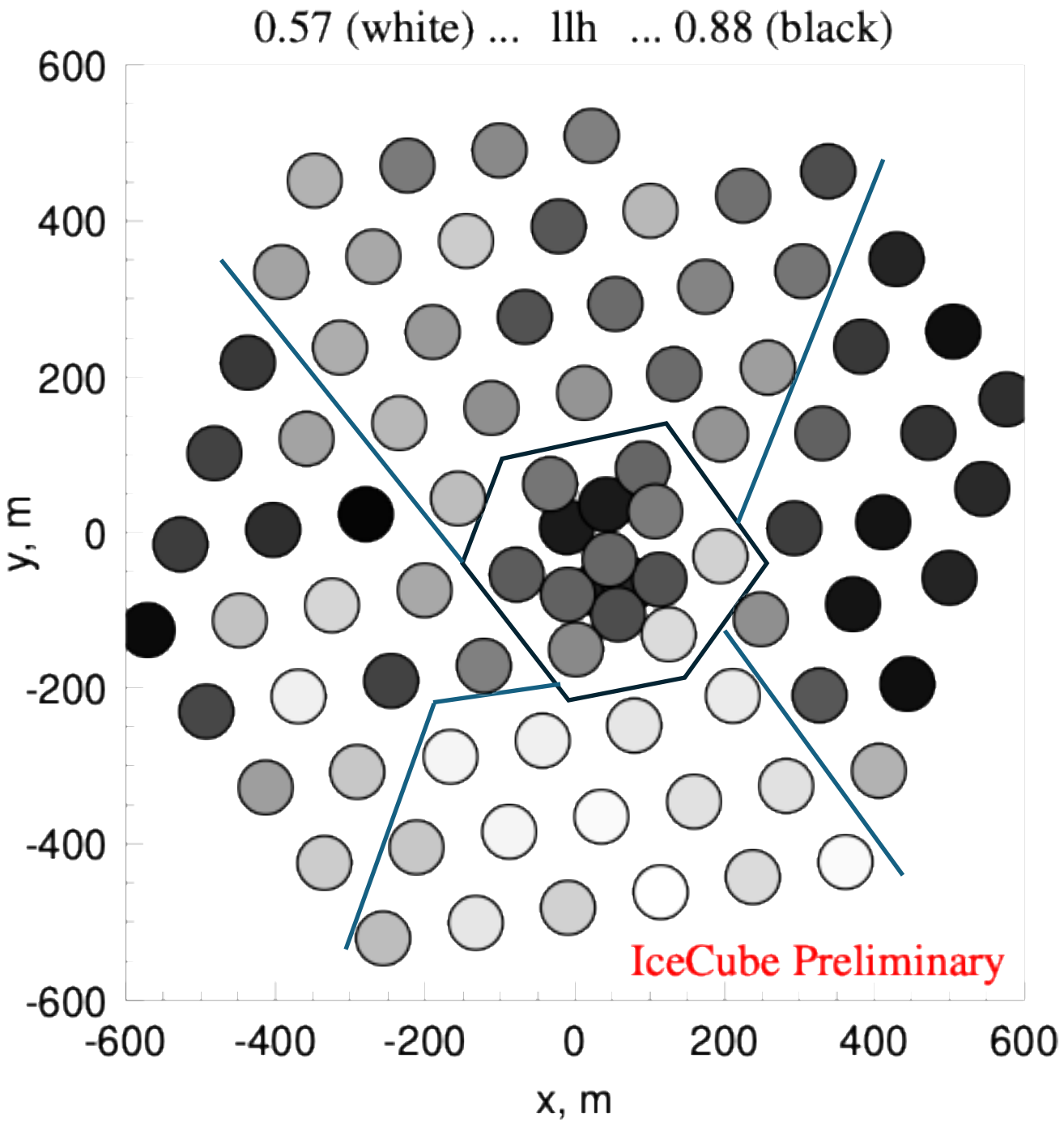
Latest ice model SPICE FTP v3 represents our latest and best understanding of the IceCube ice.

It incorporates the birefringence model of anisotropy from the previous model SPICE BFR, refines our model of the scattering function, and describes ice layer undulations everywhere in the detector with unprecedented precision.

It also comes with a full covariance matrix and thus a model of statistical uncertainties. However, the g.o.f. improvements from the previous ice model (BFR) go far beyond what is expected from these uncertainties, and thus a question was raised: how much more improvement is possible.

We simulated the complete flasher dataset with the best ice and detector description. The g.o.f. and model error, calculated in the same way as for data, are indicated as “statistical floor”.





Uniformity in quality of detector description

Average llh (over all LEDs) on each string.

Overall average for the entire detector is 0.664

Cf. reconstruction of simulated data:

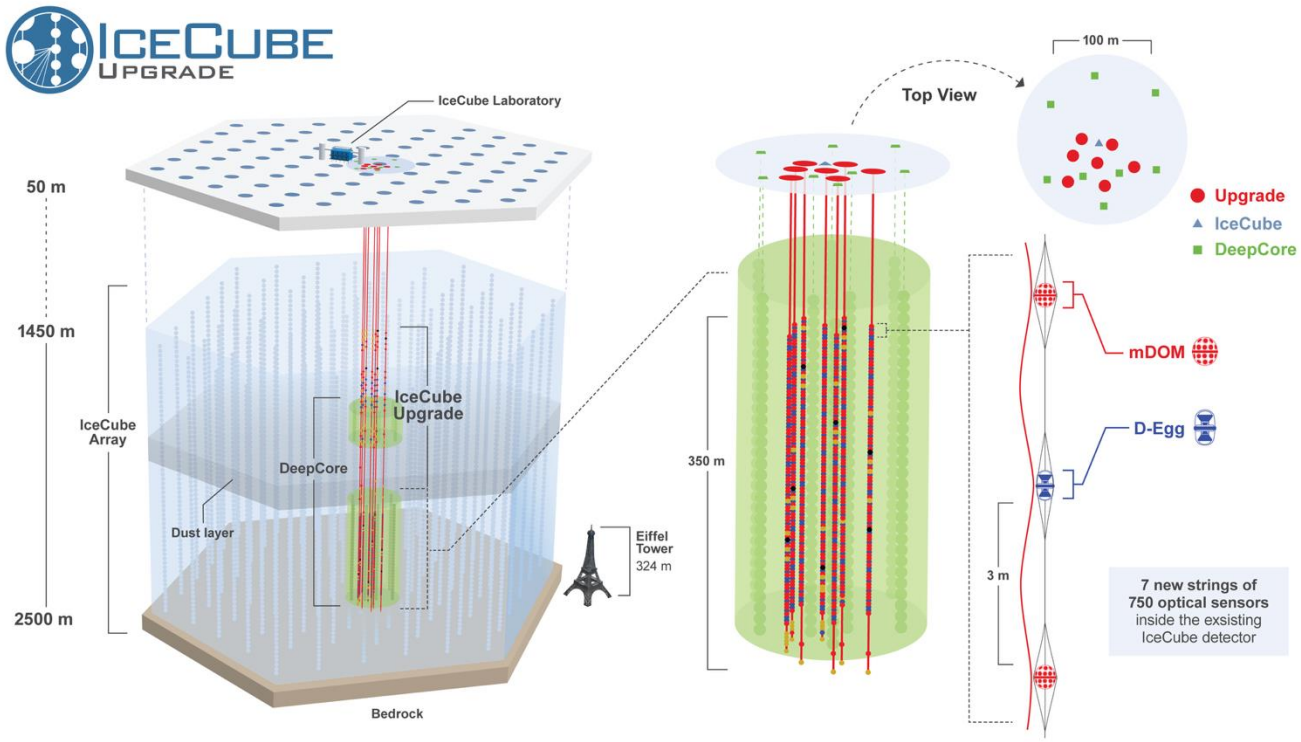
range of 0.42 to 0.45 with the average of 0.439.

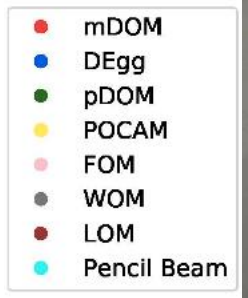
Quality of description of data is worse than simulated data everywhere but also varies in different parts of the detector.

This is seen in a variety of metrics (flasher LED brightness, DOM sensitivity, hole ice quality)

Not explained by deployment order or time/fuel spent on string deployment

IceCube Upgrade



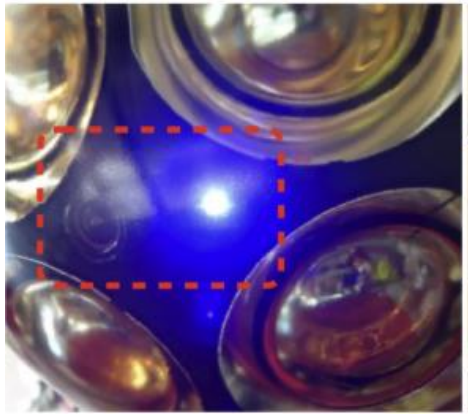




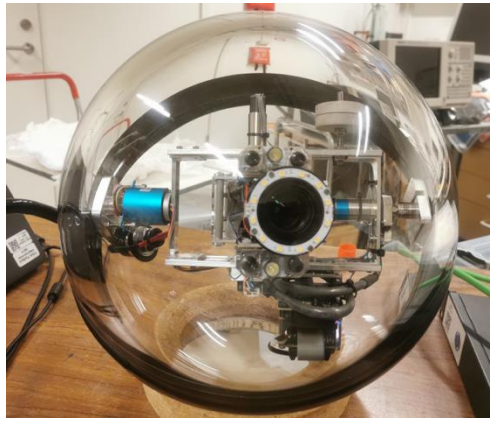


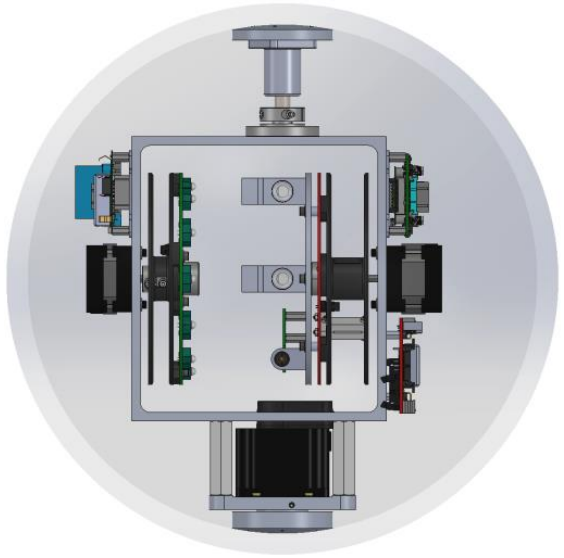


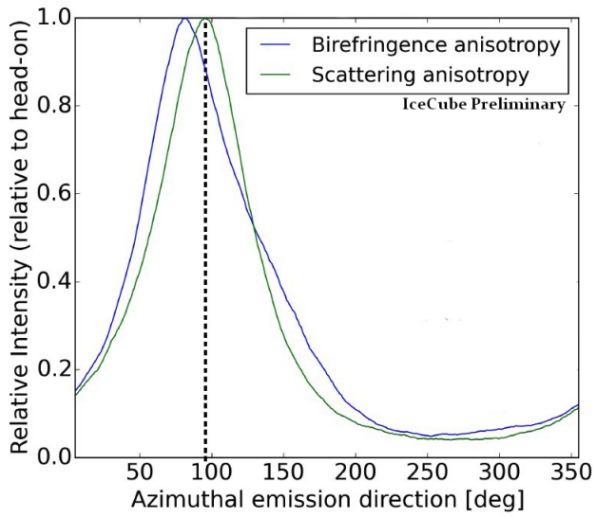












Summary and Outlook

Much progress over 30 years

From air bubbles in AMANDA-A to ice anisotropy due to birefringent ice crystals

Improvements can be gauged with llh, model error, and average waveform plot

We have a full description of statistical uncertainties of ice layer properties

However, interpretation of uncertainties is complicated since we have not yet reached the statistical floor

Are we still missing a major piece of the ice model puzzle?

Special calibration devices in IceCube Upgrade may shed light on this.

Why do we care about ice

IceCube detector uses Antarctic ice as its detection medium

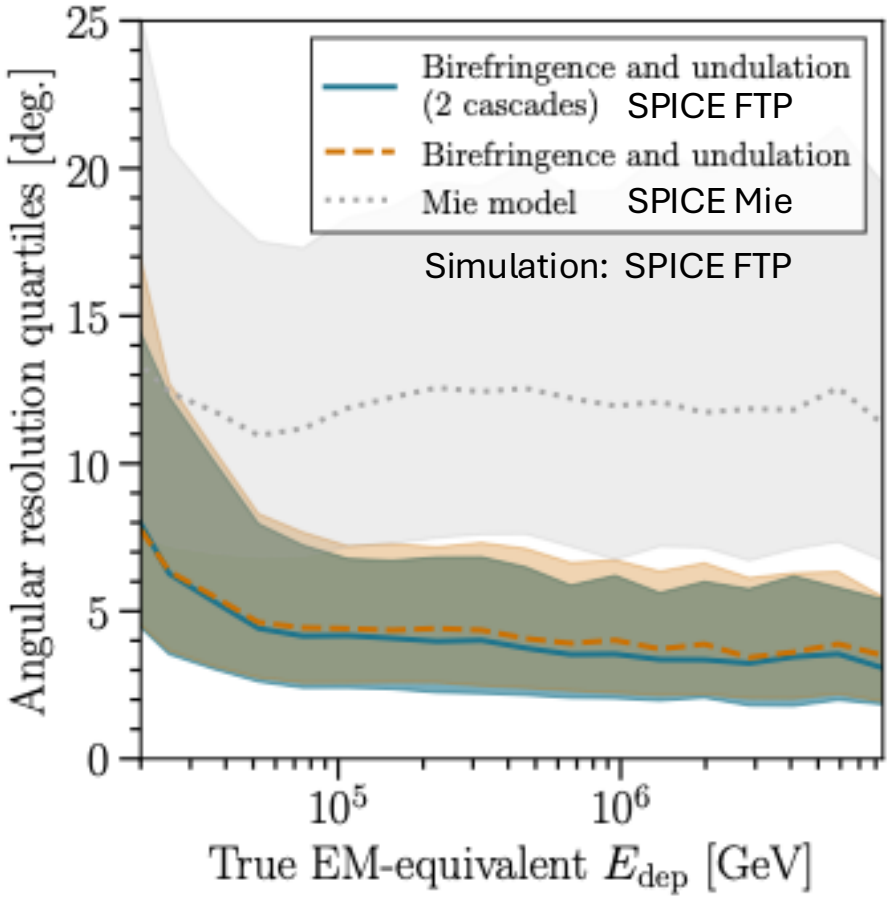
Charged particles moving through its volume generate Cherenkov light

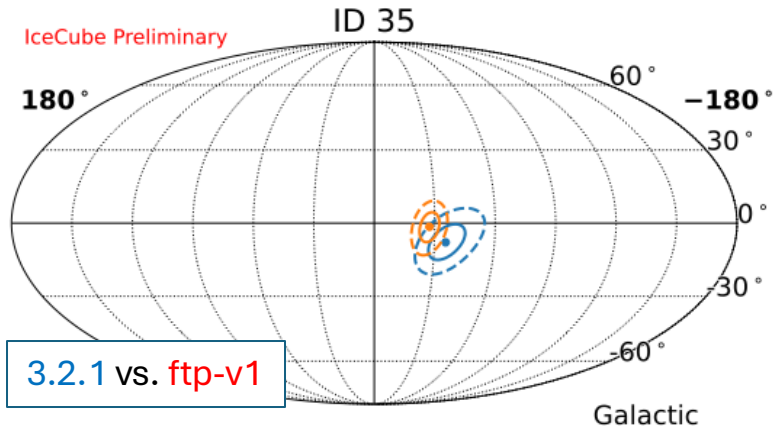
Need to describe light propagation in both simulation and event reconstruction

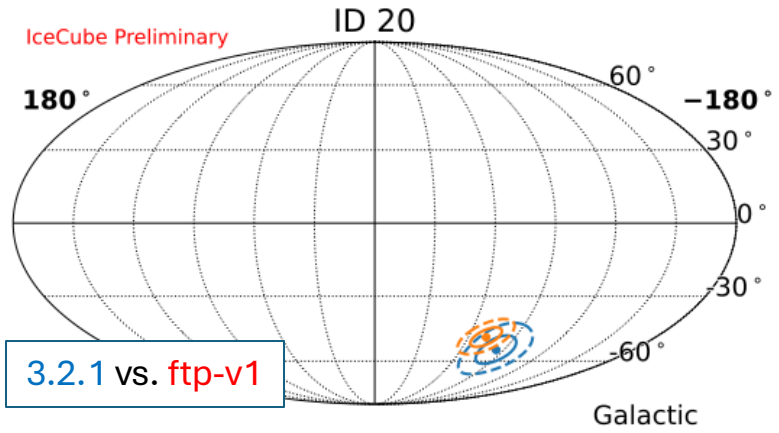
This is a major source of systematic uncertainties of IceCube analyses

Links to other fields: glaciology, climate science

Impact of ice improvements to data analysis





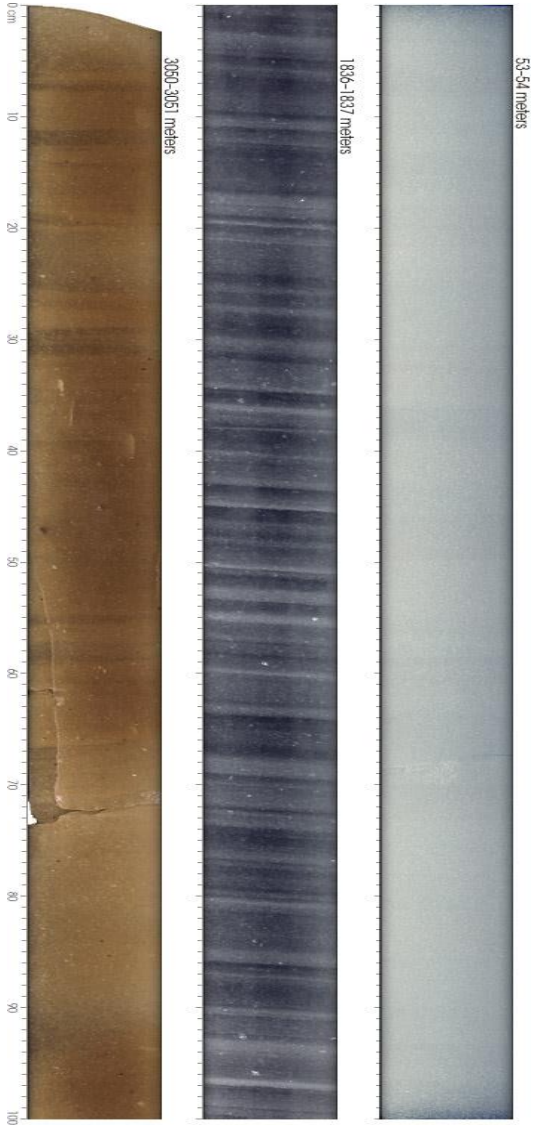


For data simulated with the best current ice model a large improvement is observed in angular resolution of reconstructed cascade directions with the same ice vs. older model.

For real data (2 HESE cascades shown above), systematic shifts may go beyond statistical uncertainties as seen from the updated ice model.

As we get closer to the statistical floor with our ice model description, we gain more confidence that the reconstruction direction and associated uncertainty contours are accurate.

Timeline



AMANDA ice models:			model error
bulk, f125, mam, mamint, stdkurt, sudkurt, kgm, …			
millennium (published 2006) → AHA (2007)			55%
IceCube ice models:			
WHAM	(2011)		42%
SPICE 1	(2009)		29%
SPICE 2, 2+, 2x, 2y	(2010)	added ice layer tilt	
SPICE Mie	(2011)	fit to scattering function	29%
SPICE Lea	(2012)	fit to scattering anisotropy	20%
SPICE (Munich)	(2013)	7-string, LED unfolding	17%
SPICE^3 (CUBE)	(2014)	llh fixes, DOM sensitivity fits	11%
SPICE 3.0	(2015)	improved RDE, ang. sens. fits	10%
SPICE 3.1, 3.2	(2016)	85-string, correlated model fit	<10%
SPICE HD, 3.2.2	(2017)	direct HI and DOM sens., cable, DOM tilt	
SPICE EMRM	(2018)	absorption-based anisotropy	*single*
SPICE BFR (v1, v2)	(2020)	birefringence-based anisotropy	*LEDs*
SPICE FTP (v0, v1)	(2022)	precise fit to tilt across detector volume	
SPICE FTP (v2, v3)	(2023)	w/precise covariance matrix calculation	

Model error (precision in charge prediction): <10%
Extrapolation uncertainty: 13% (sca) / 15% (abs)
Linearity: < 2% in range 0.1 … 500 p.e.

llh and model error

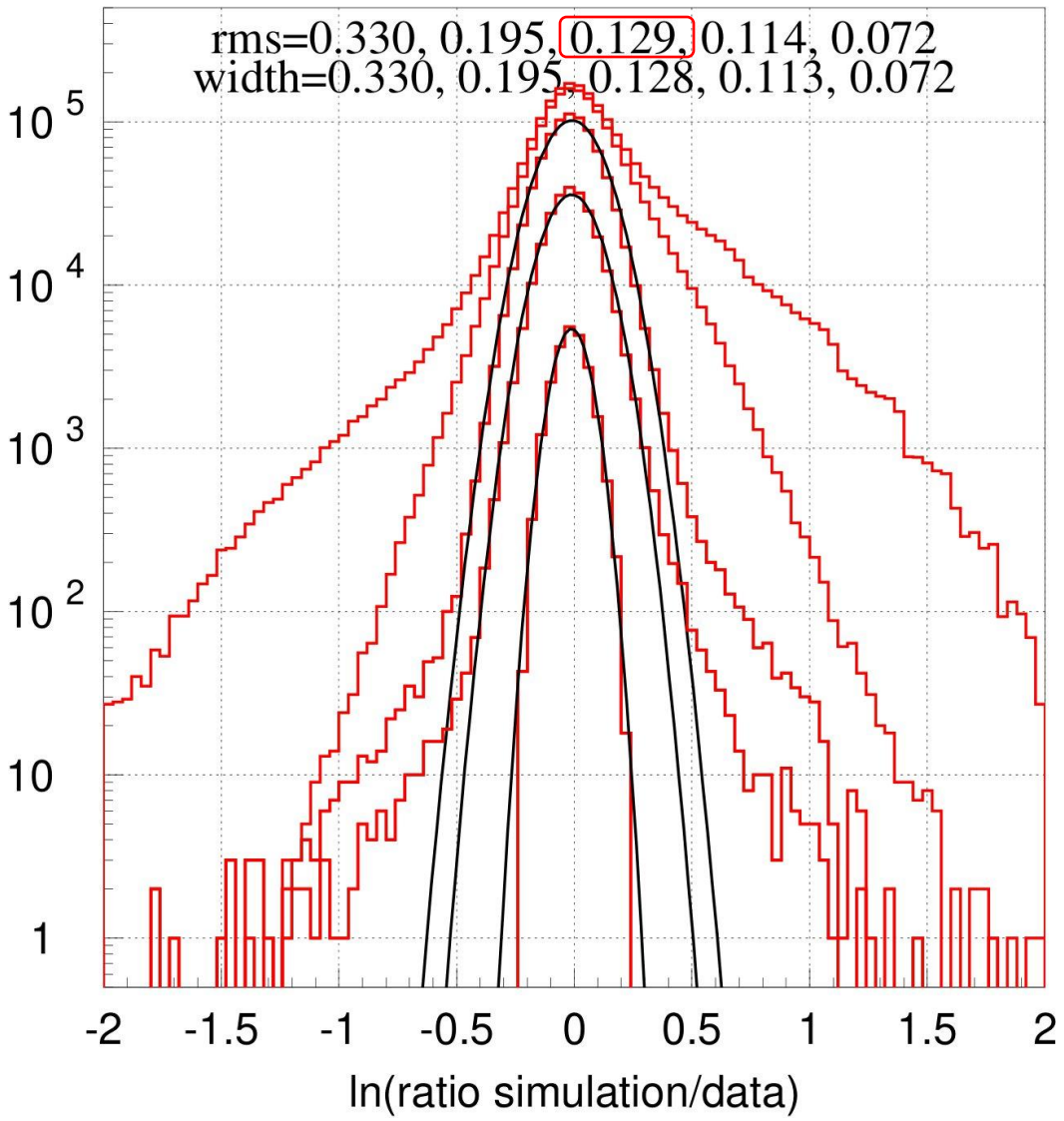
The quantity that we use during the fit is “llh”, which is constructed as a saturated Poisson likelihood for data and simulation with their expectation values compared with the “model error term”:

$$\frac{P(\text{same process})}{P(\text{independent processes})} = \left(\frac{\mu_s}{s/n_s}\right)^s \cdot \left(\frac{\mu_d}{d/n_d}\right)^d \cdot \exp\frac{\ln^2(\mu_d/\mu_s)}{-2\sigma^2}$$

For each flasher LED configuration, this quantity is summed over Bayesian-blocked time bins in receiving DOMs and normalized by their number. Then this normalized quantity is summed for all flasher configurations (of which we have 60614 – 12 LEDs times 5160 DOMs minus broken and cDOMs and minus some failed LEDs).

We have made multiple improvements to llh over the years, with each new ice model much better than the previous one. Naturally, a question arises: how far are we from the best possible llh? Say, if the physics of flasher LED events is modeled perfectly, in the absence of any (known or unknown) systematic uncertainties, what is the expected value of the llh? We can refer to such a value as a “statistical floor” of llh.

Model error

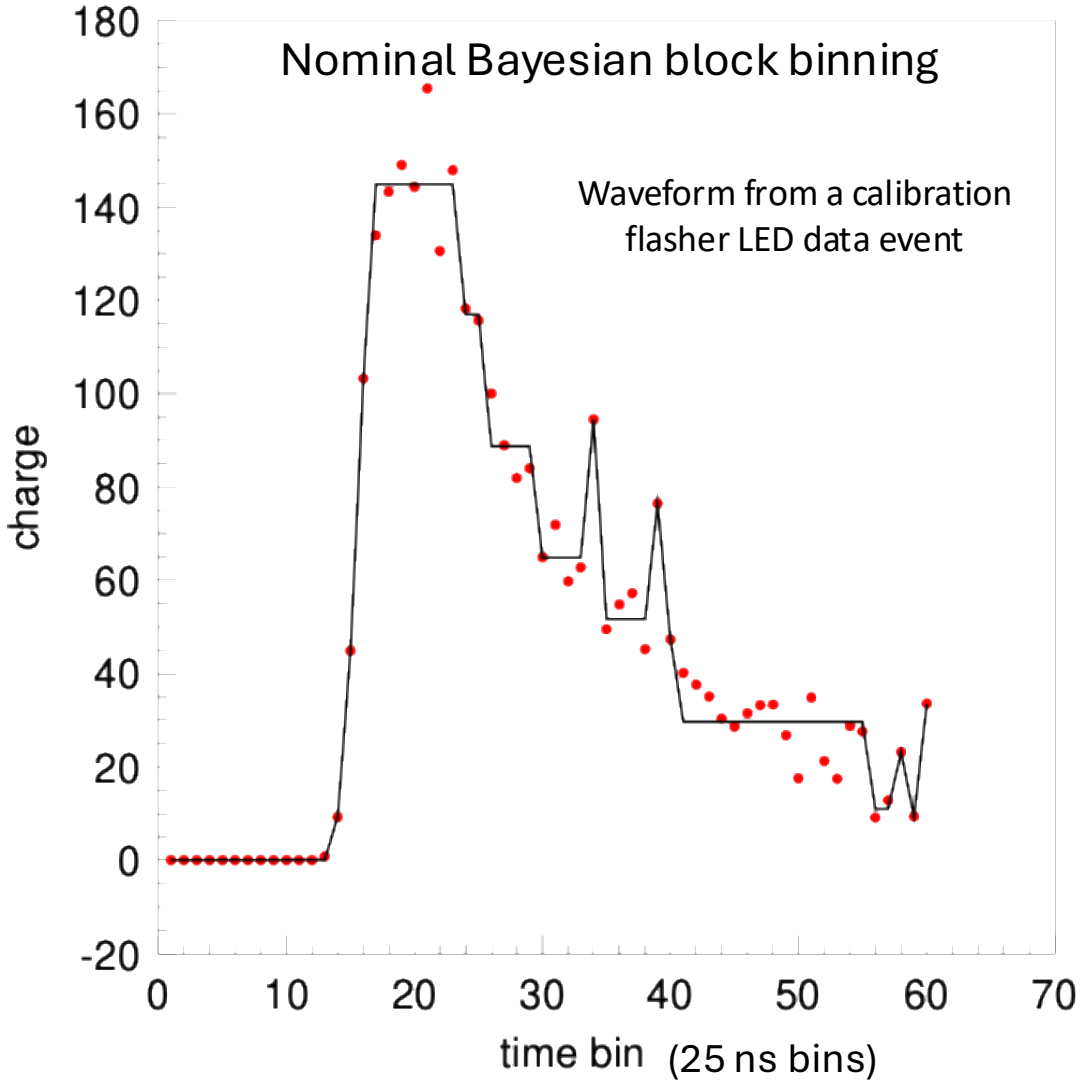


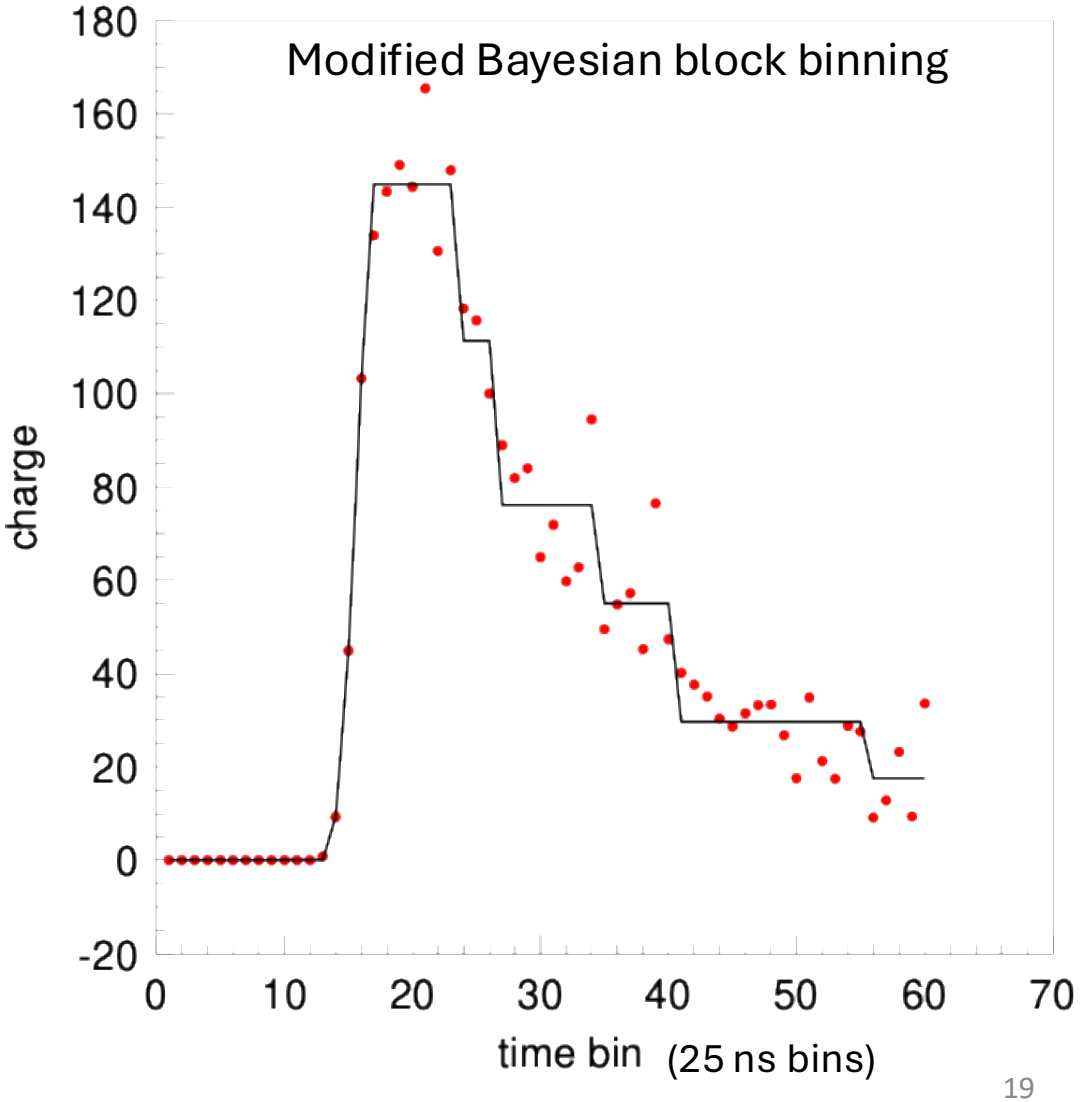
The size of σ in the model error term in the llh construction is estimated from plots as shown here. A logarithm of charge ratio in simulation over data is histogrammed for all receiving DOMs for all flasher configurations. The charge we use in this construction is integrated over the time window used by this analysis (i.e., full charge per receiving DOM).

The plot shows 5 histograms (with their rms and width of fitted gaussian listed in the caption) for different threshold value of accepted charge: (1) no cut, (2) 1 p.e., (3) 10 p.e., (4) 100 p.e., and (5) 400 p.e.

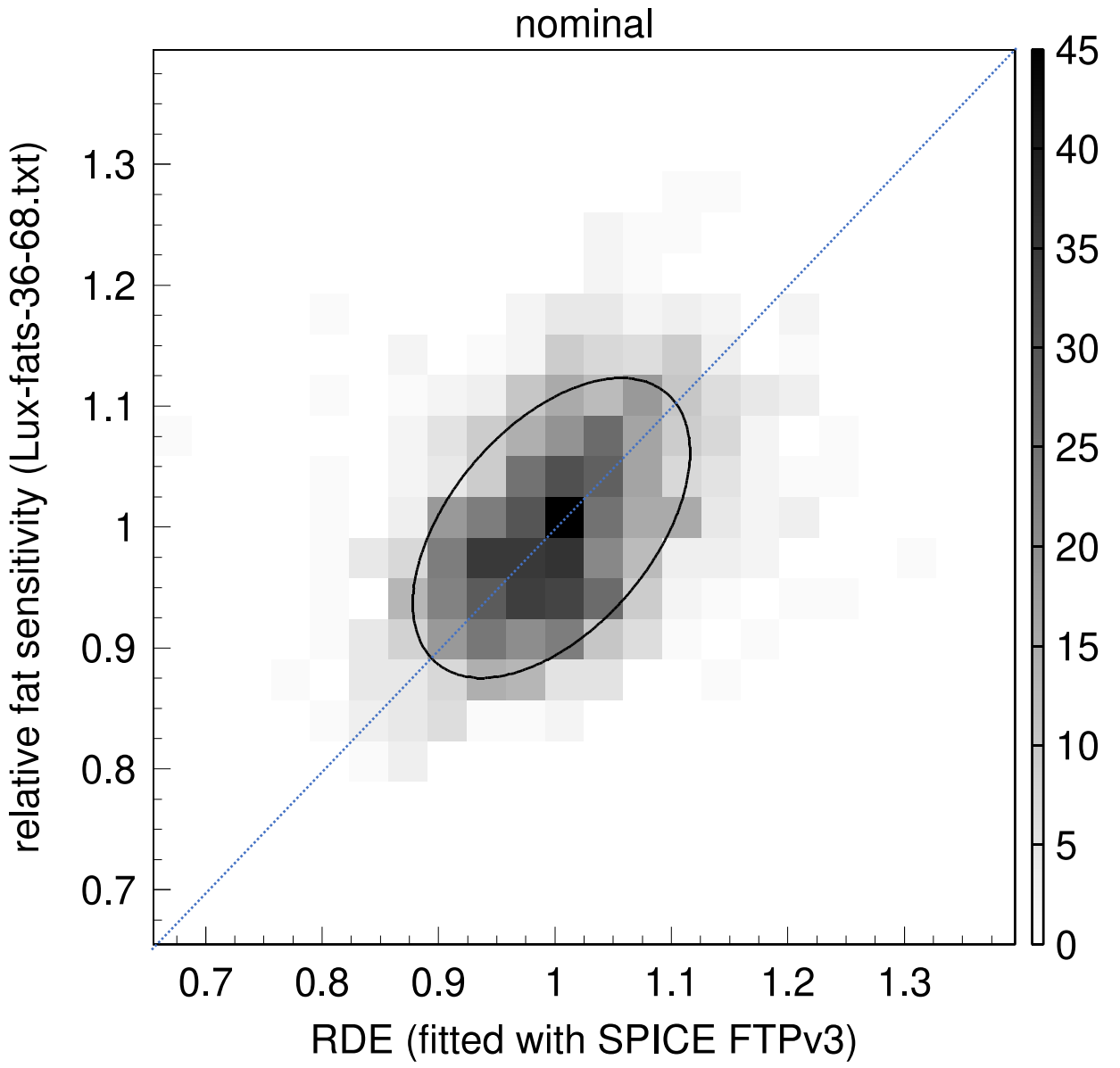
The rms/width at each threshold level depends on statistics of data and simulation (i.e., how many events in data and simulation for each configuration). Typically, data has more than 100 events, while simulation (shown here) has only 10. We usually take the middle value (10 p.e. cut – 12.9% here). This number will reduce to 11.8% for 100 simulated events. We had previously estimated (for SPICE 3.2) that after subtracting statistical contribution the model error is 9.8%.

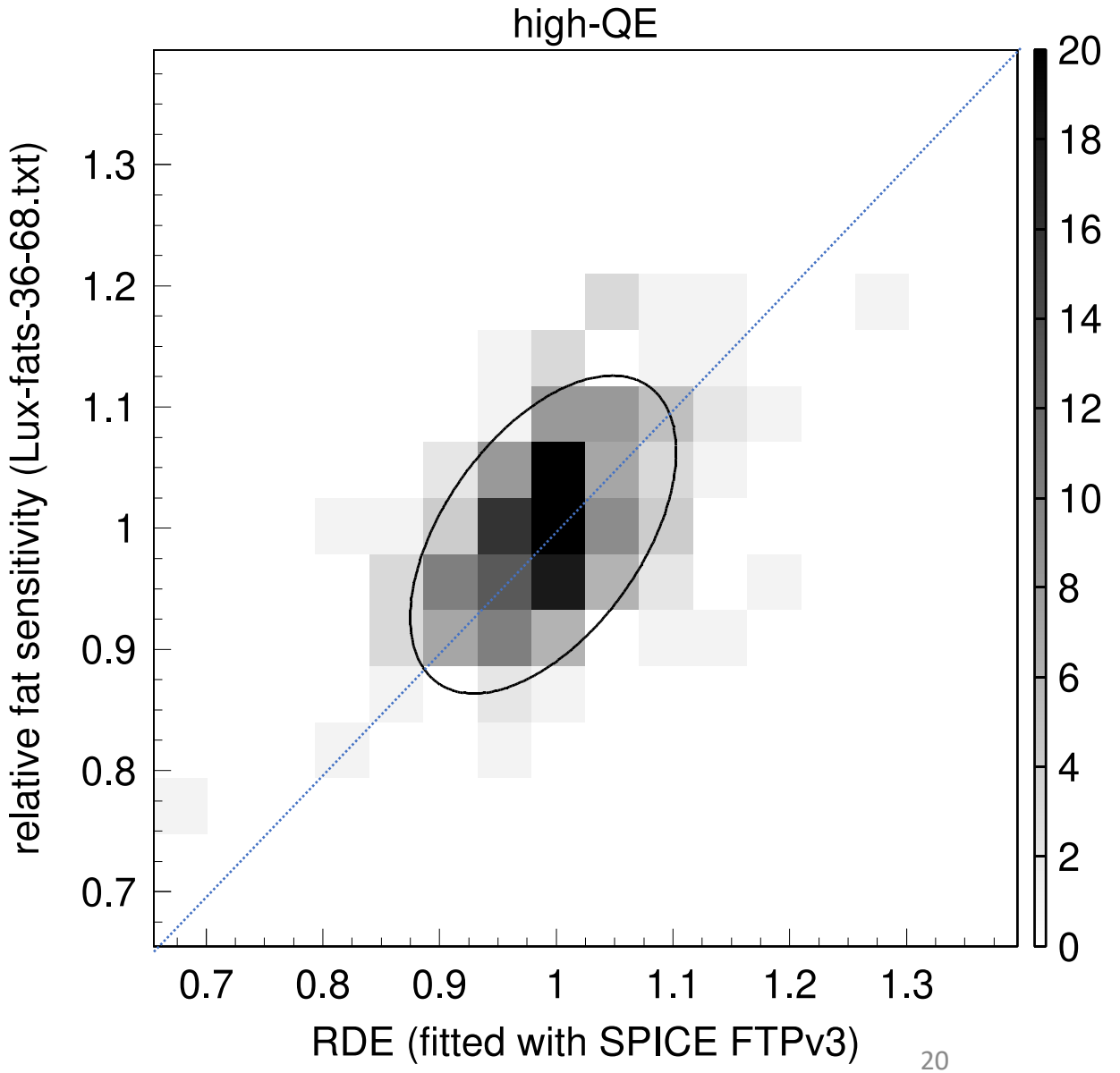
Time waveform binning



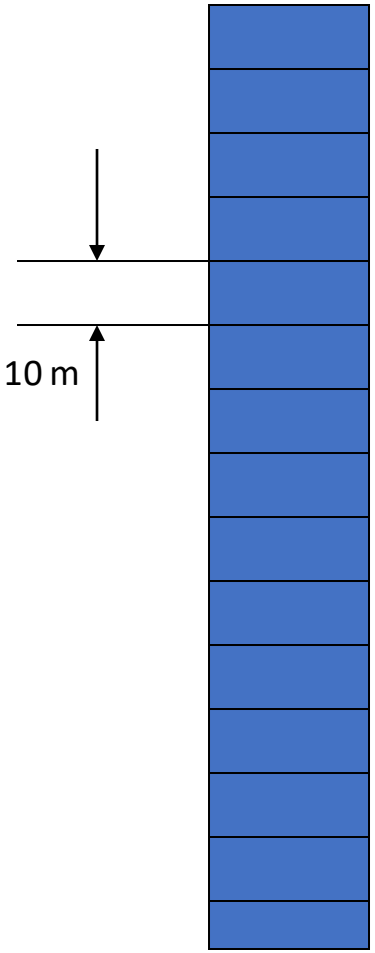


Relative in-ice DOM efficiencies: correlation to FAT





Ice layer parametrization



In each 10-meter layer define:

- scattering
- absorption
- ice crystal density



scattering



Source is blurred

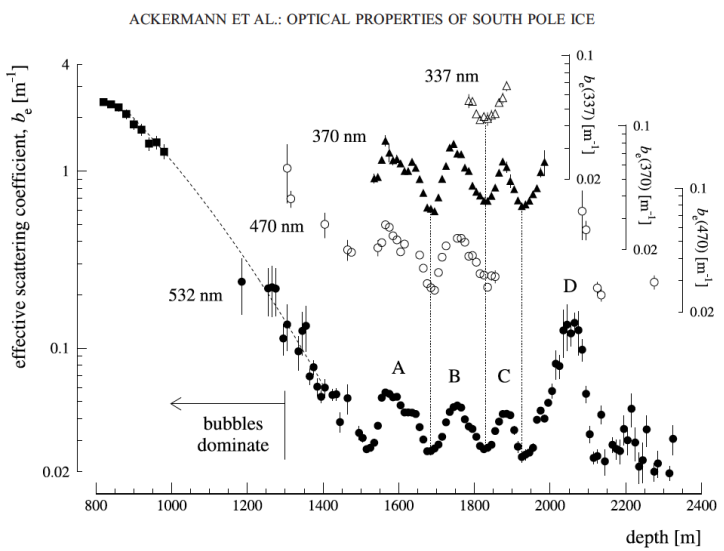
absorption

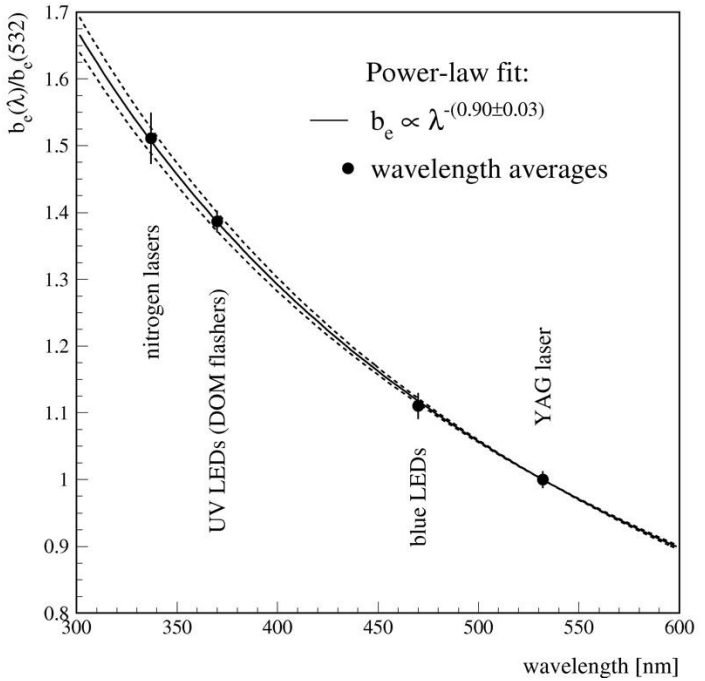


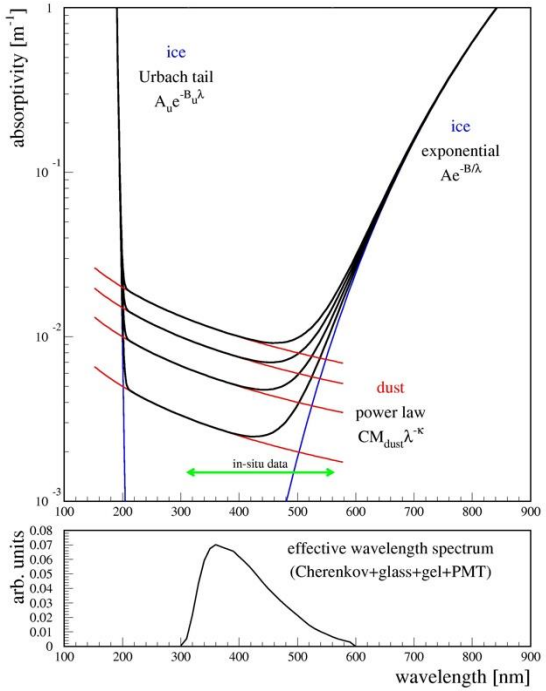
Source is dimmer

a = inverse absorption length ($1/\lambda_{abs}$)
b = inverse scattering length ($1/\lambda_{sca}$)

AMANDA-II: comprehensive ice model

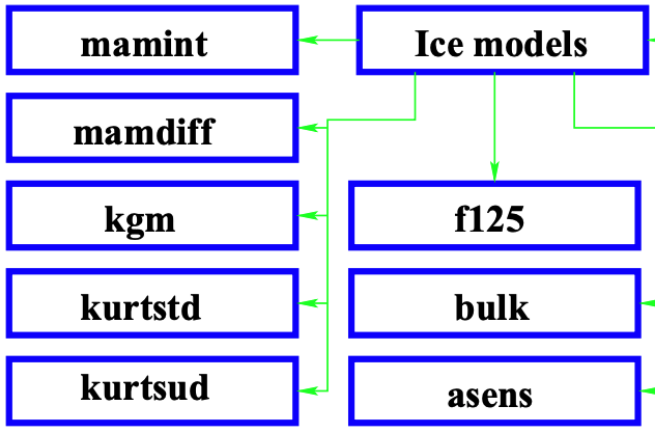




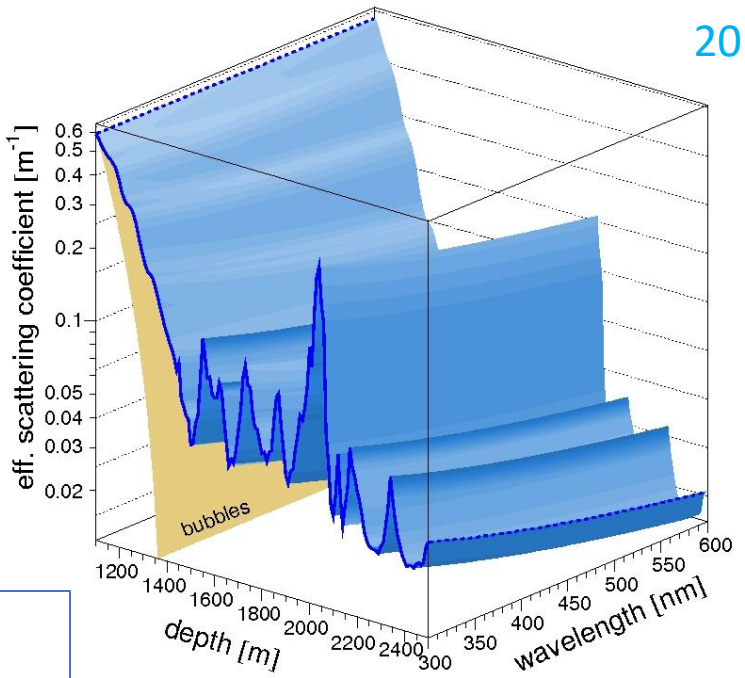


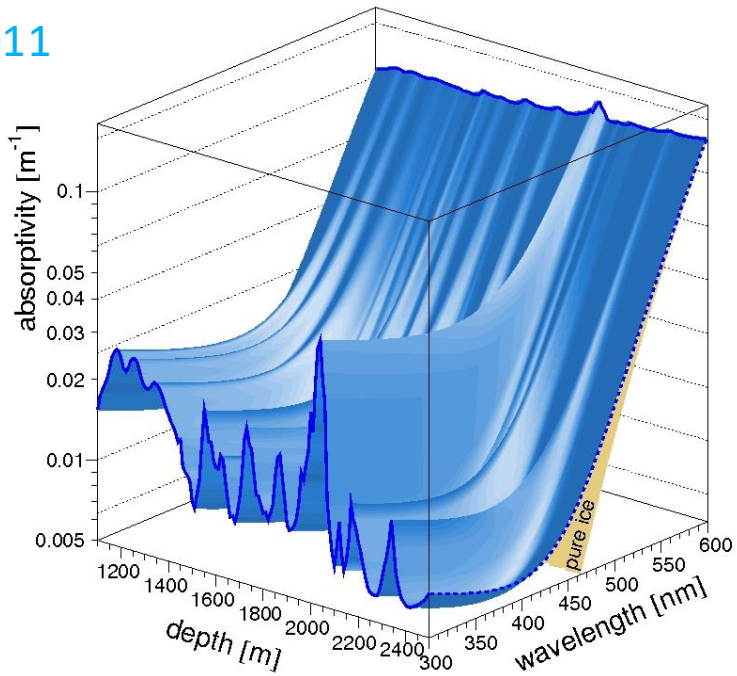
Ice is extremely transparent between 200 nm and 500 nm at depths below 1350 m
Scattering and absorption are determined by dust concentration
Wavelength dependence of dust scattering and absorption follow power law
Wavelength dependence was verified with IceCube, but is still used basically unchanged

AMANDA-era ice models



2011





Kurt
KGM (Kurt-Gary)
MAM (modified absorption)
Millennium/Y2K

1995-2003

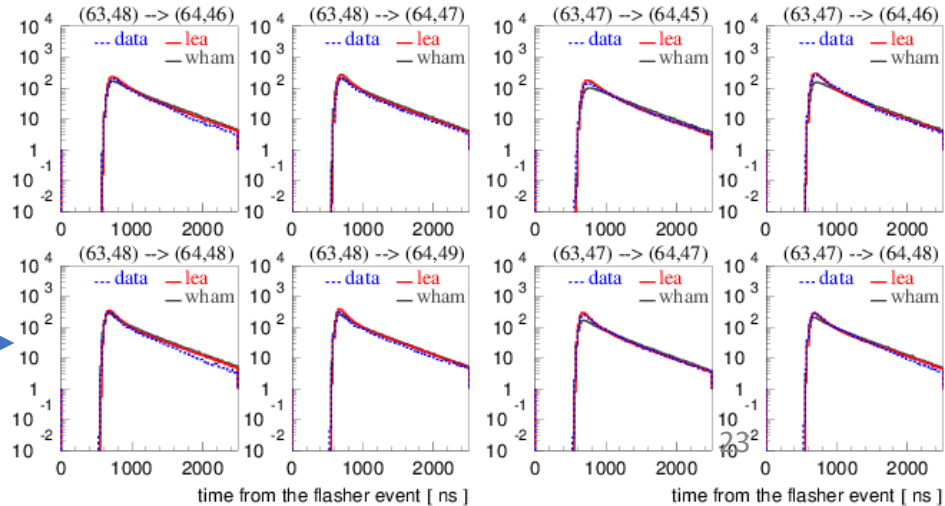
AHA 2006-2007

Lordi

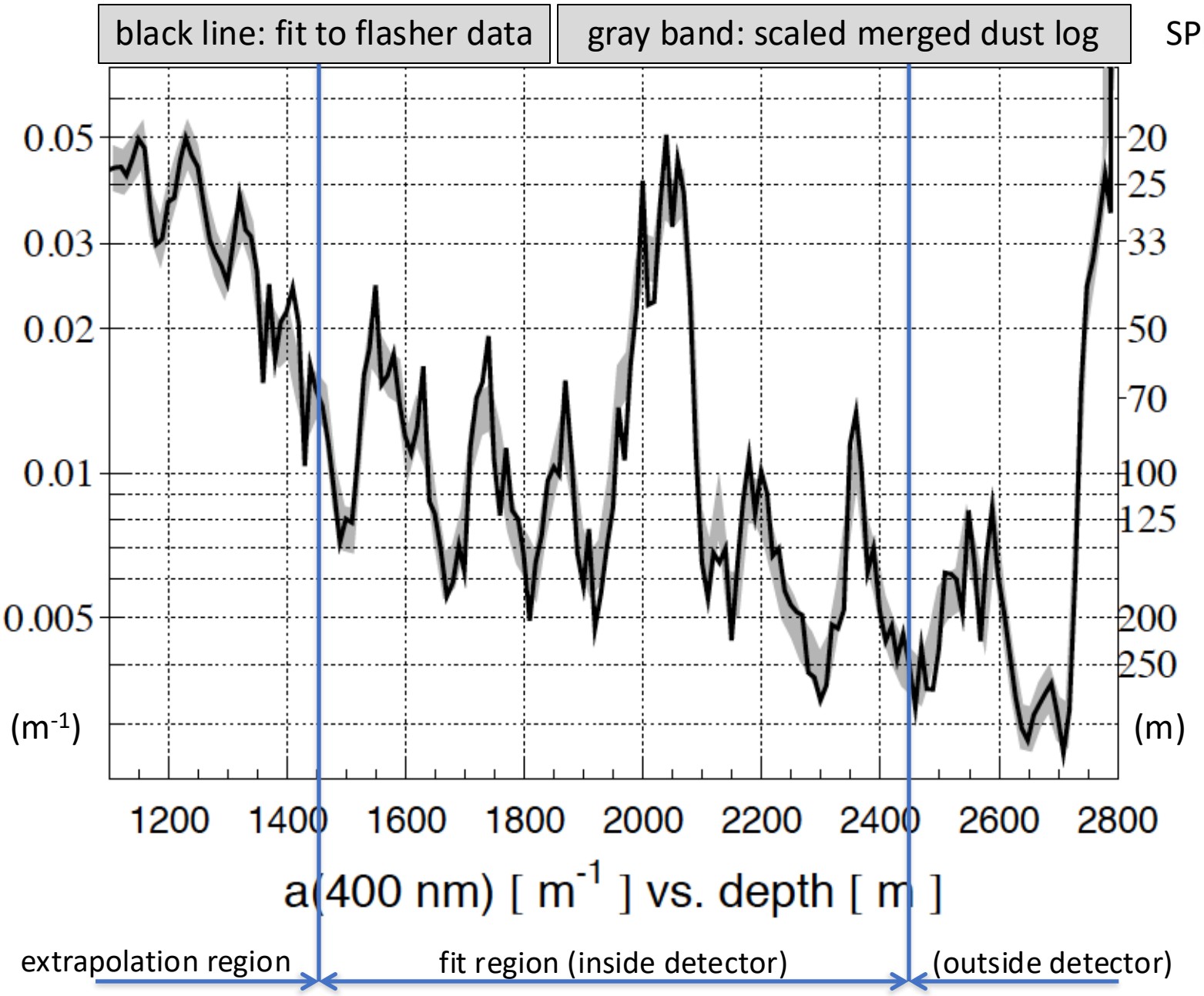
WHAM! (Water Hardened Antarctic Measurement)

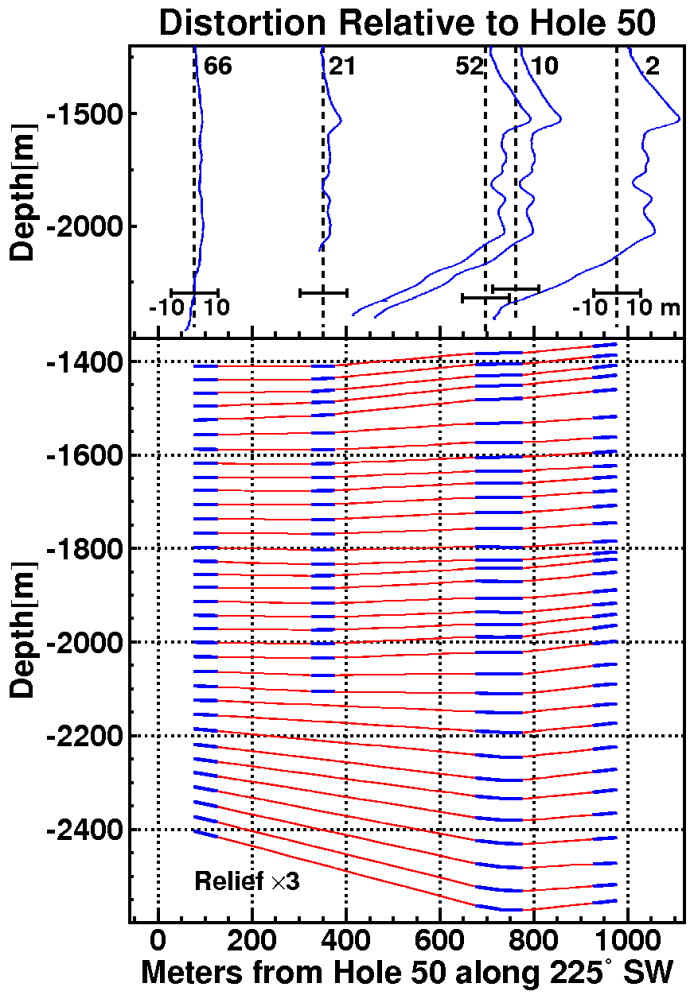
Models with an IceCube wiki page

Comparison with SPICE family (lea)

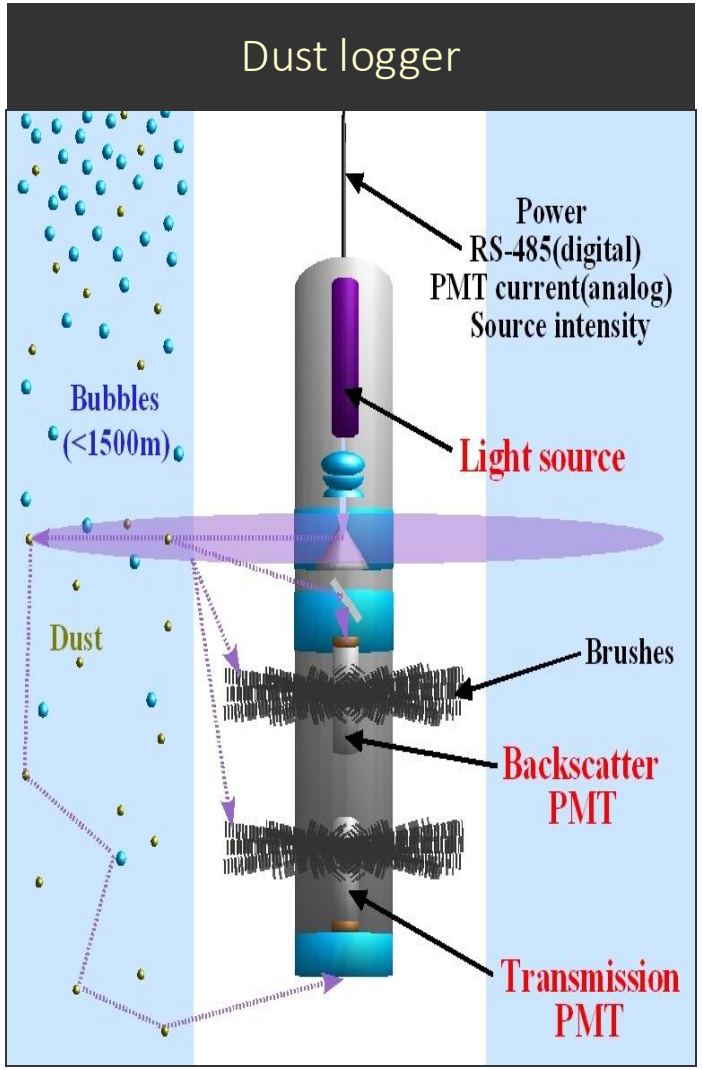


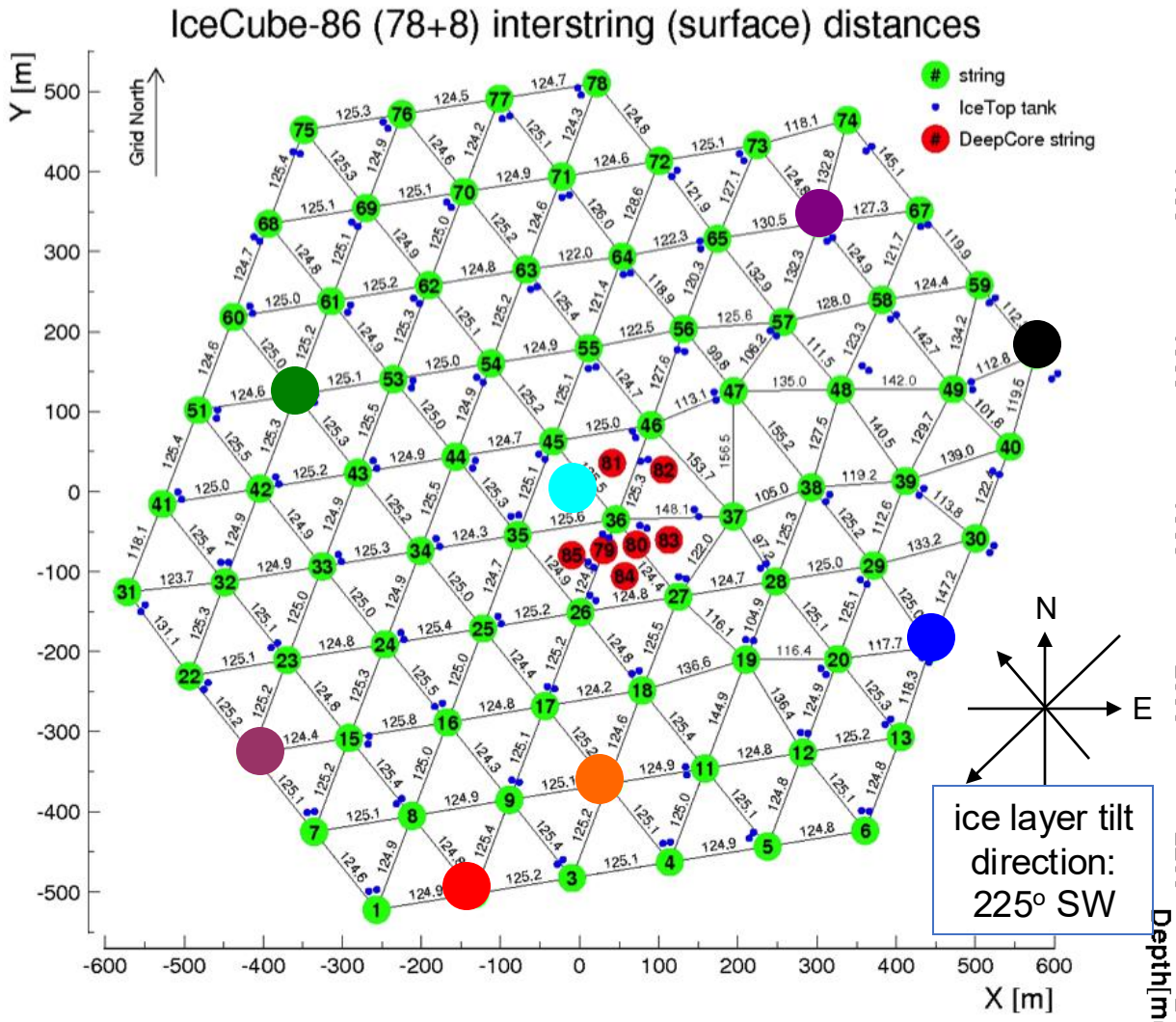
Correlation of fitted optical properties with dust logger data

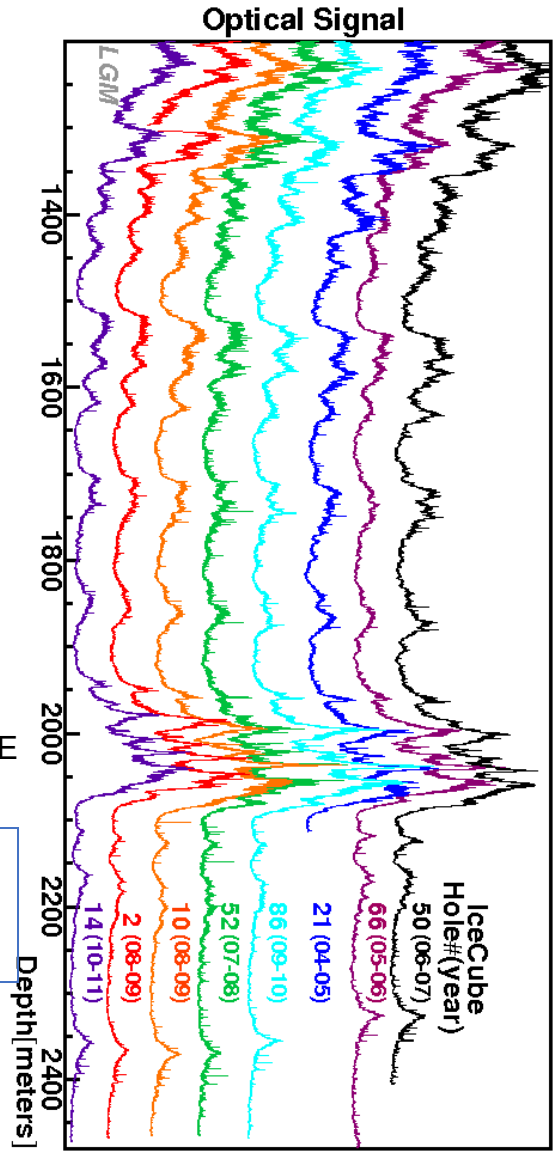




Dust logger mapping of the ice tilt





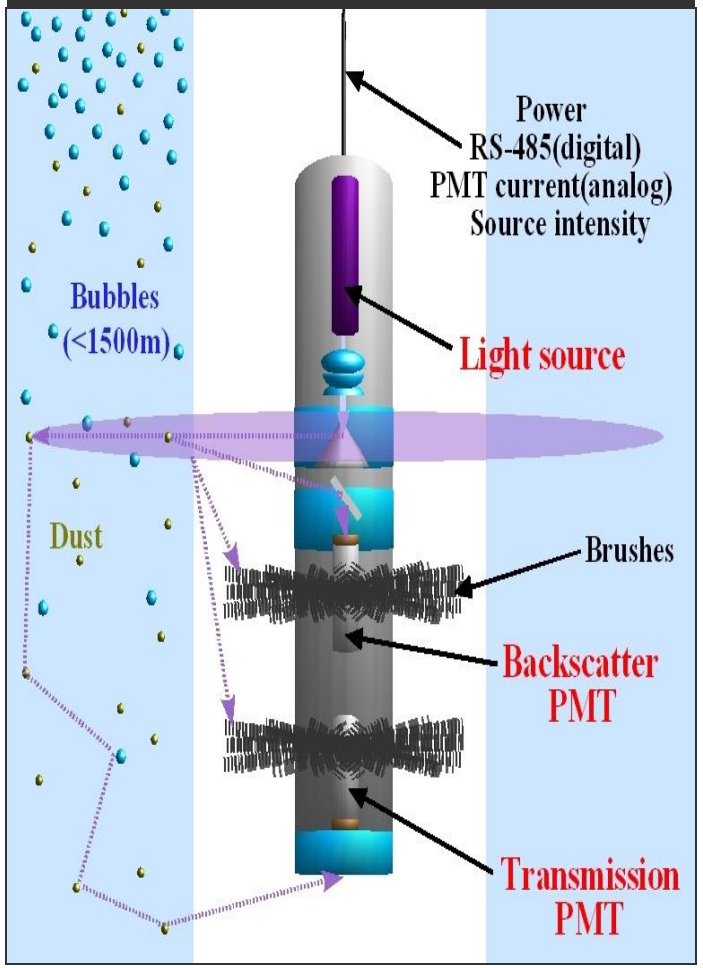


The ice layers (i.e. layers of ice with similar optical properties) change in depth by as much as 60 m when going from NE to SW corners of the detector

Dust logger mapping of the ice tilt

Journal of Glaciology, Vol. 59, No. 218, 2013 doi: 10.3189/2013JoG13J068

Dust logger



South Pole glacial climate reconstruction from multi-borehole laser particulate stratigraphy

The IceCube Collaboration*

*For full author list, see Appendix

2013

ABSTRACT. The IceCube Neutrino Observatory and its prototype, AMANDA, were built in South Pole ice, using powerful hot-water drills to cleanly bore >100 holes to depths up to 2500 m. The construction of these particle physics detectors provided a unique opportunity to examine the deep ice sheet using a variety of novel techniques. We made high-resolution particulate profiles with a laser dust logger in eight of the boreholes during detector commissioning between 2004 and 2010. The South Pole laser logs are among the most clearly resolved measurements of Antarctic dust strata during the last glacial period and can be used to reconstruct paleoclimate records in exceptional detail. Here we use manual and algorithmic matching to synthesize our South Pole measurements with ice-core and logging data from Dome C, East Antarctica. We derive impurity concentration, precision chronology, annual-layer thickness, local spatial variability, and identify several widespread volcanic ash depositions useful for dating. We also examine the interval around ~74 ka recently isolated with radiometric dating to bracket the Toba (Sumatra) supereruption.

INTRODUCTION

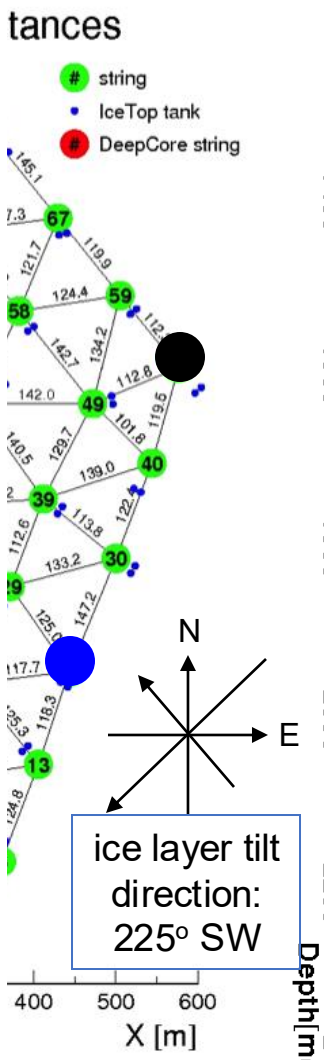
More than 50 years ago, Markov and Zheleznykh proposed using gigatons of transparent material underground as a detector of cosmic neutrinos (see Markov and Zheleznykh, 1986, and references therein). The IceCube Neutrino Observatory completed in December 2010 (IceCube Collaboration, 2006) and its predecessor, AMANDA (Antarctic Muon and Neutrino Detector Array; AMANDA Collaboration, 2001), have applied this concept in the deep ice at the South Pole to study fundamental questions in physics and astrophysics. These telescopes use large volumes of ice to observe the subatomic charged particles produced by energetic neutrinos, that have fortuitously interacted via the weak force with nucleons in the ice near the detector. Muons, hadronic cascades and electromagnetic cascades generated by the neutrinos can be tracked via charged-particle Cherenkov radiation at ultraviolet and visible wavelengths with an embedded matrix of sensitive photomultipliers. The density of sensors and size of the instrumented volume determine the threshold, resolution and practicably attainable upper limit of detected neutrino energies. Since the spectrum of cosmic neutrinos is presumed to roughly follow that of cosmic rays and fall steeply with energy, IceCube was designed at the kilometer scale to detect small fluxes of neutrinos in the 1 TeV to 1 PeV energy range over the lifetime of the experiment.

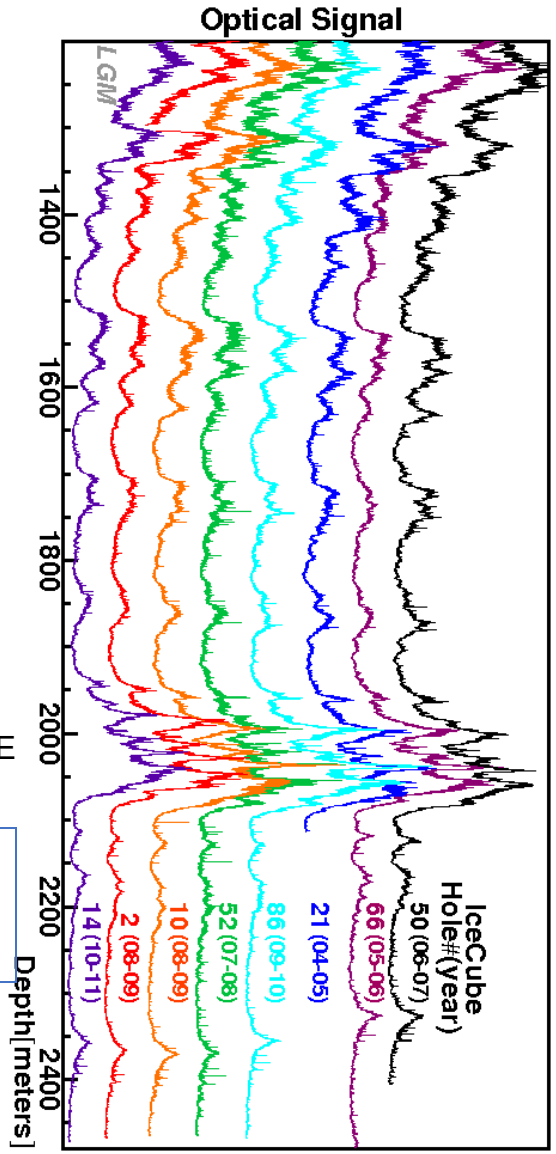
The buried component of IceCube consists of 5160 photomultiplier tubes, frozen into 86 boreholes and arrayed over 1 km^3 from 1450 m to 2450 m depth (IceCube Collaboration, 2009). IceCube and AMANDA rely on the extreme clarity of Antarctic ice, at sufficient depths that all residual air bubbles originally trapped in surface snow have converted to hydrates. Air clathrate hydrate crystals have almost exactly the same refractive index as ice ($\Delta n/n \approx 4 \times 10^{-3}$; Uchida and others, 1995) and so are

out a painstaking analysis of fresh Vostok ice-core samples, crucially, within a few weeks of coring and before the hydrates could revert back to air bubbles upon relaxation at the surface. Their work (Barkov and Lipenkov, 1985) presaged our discovery that South Pole ice is still bubbly at depths shallower than 1300 m. Bubble scattering prevented accurate directional reconstruction, and AMANDA-A was mainly effective as a subatomic particle calorimeter (Askebjer and others, 1995) but not as a telescope. Bubbles decrease in size with depth but persist until at least ~1350 m at South Pole, and to comparable or greater depths at every location we have studied in the interiors of Antarctica and Greenland.

IceCube construction depended critically on the drilling team and the 5 MW Enhanced Hot-Water Drill (EHWD), capable of boring 20 holes, each 2500 m deep and 60 cm in diameter, in a 2 month season. This massive ice-drilling project has enabled us to investigate South Pole ice and create synergies with other disciplines. Our studies to date include precision measurements of optical properties (Woschnagg and Price, 2001; Ackermann and others, 2006; IceCube Collaboration, 2013); acoustic properties (IceCube Collaboration, 2010, 2011); glaciological properties such as flow, shear and temperature (Price and others, 2002); and paleoclimatology, including a reconstruction of surface roughness as a proxy for cyclonic activity (Bay and others, 2010).

A principal aspect of calibrating the IceCube detector has been to map scattering and absorption of light in the deep ice. Bubble-free Antarctic ice is the purest natural solid on Earth, and the most transparent at ultraviolet to visible wavelengths. Photons with wavelengths shorter than ~200 nm are strongly attenuated by electronic absorption in water; for wavelengths longer than ~600 nm, molecular absorption dominates. Between 200 and 600 nm, transmis-





The ice layers (i.e. layers o … as much as 60 m wh … epth by …

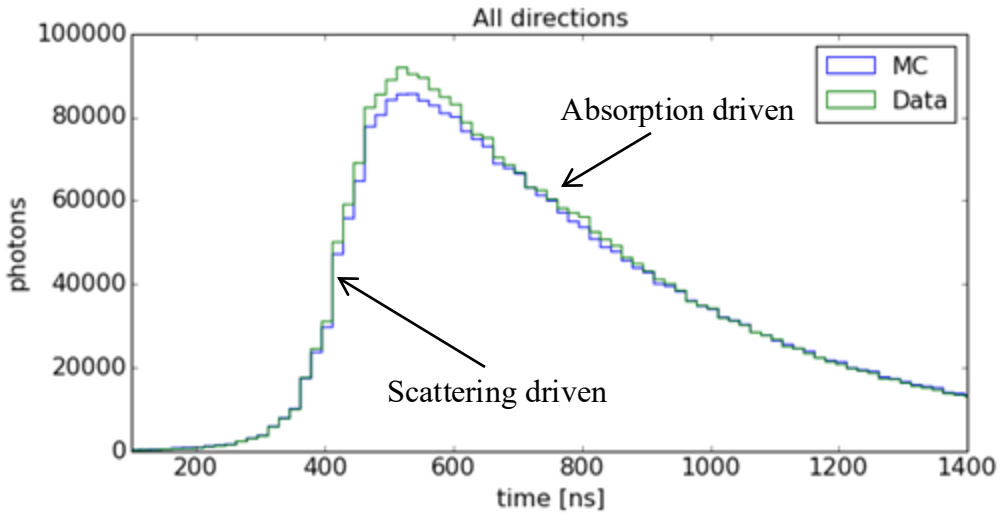
Models of optical ice anisotropy in IceCube

1. Scattering (mainly): direction dependent scattering function (ICRC 2013)
2. Absorption (mainly): direction dependent absorption (studied in 2018)

Introduced depth-dependence (2017)

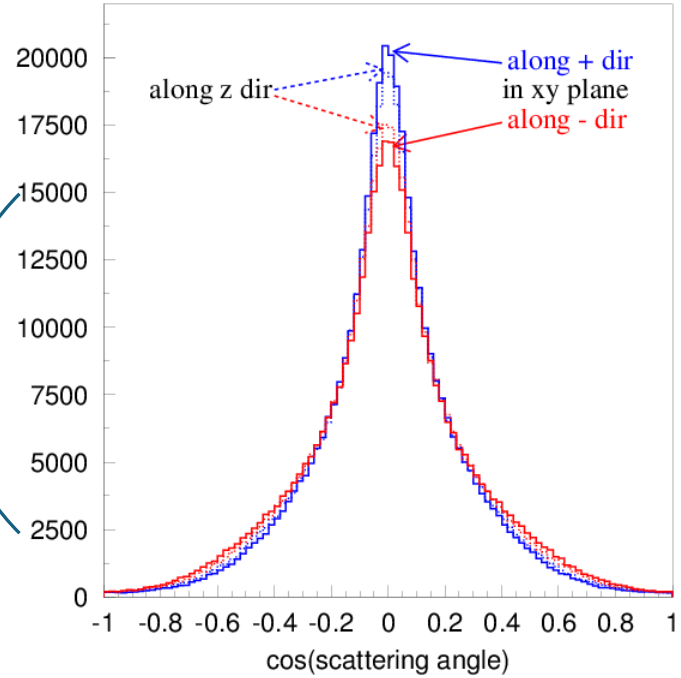
Discrepancies between data and simulation remain

Cannot simultaneously fit total charge and
arrival time distribution to statistical precision



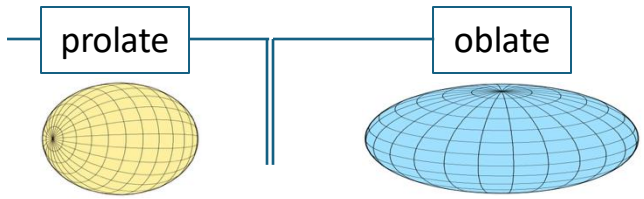
scattering-based

SPICE Lea, 3.2.x



absorption-based

SPICE EMRM



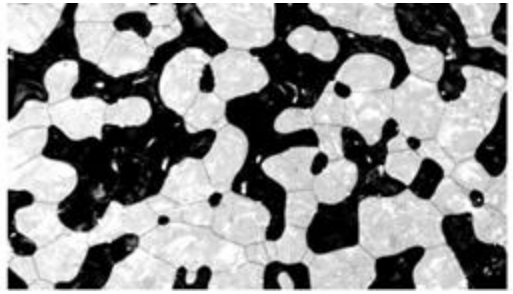
Scattering patterns birefringent ice

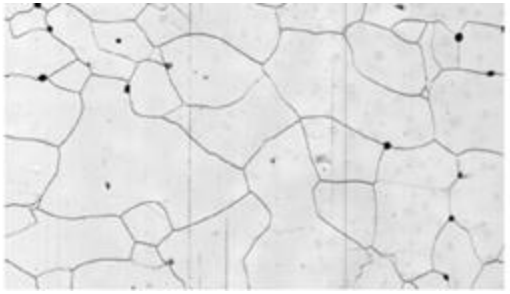
Running MC simulation with realistic crystal size, elongation, and orientation distributions (correlated to flow direction):

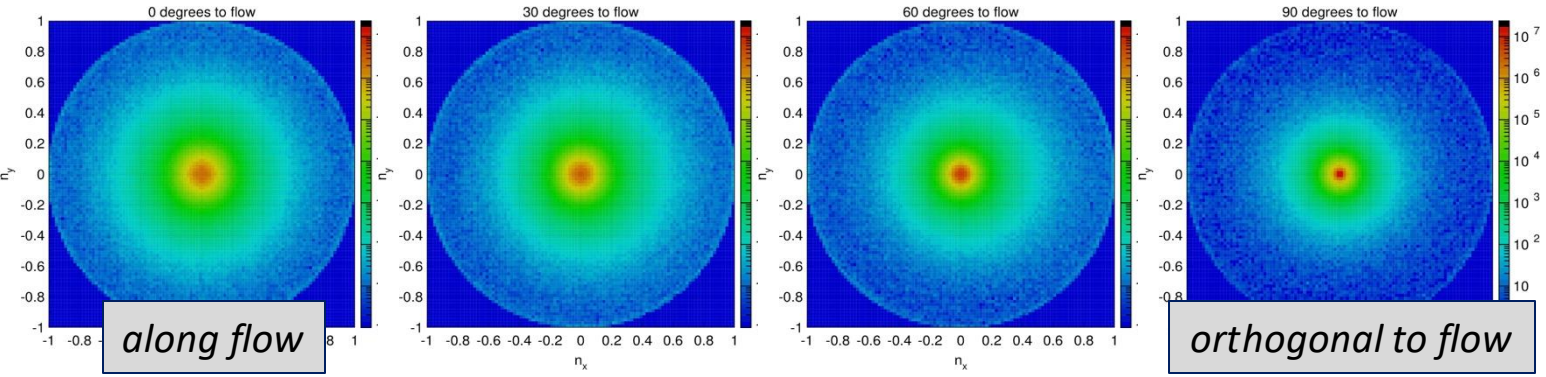
Diffusion is largest on flow axis and smallest orthogonal to it

Photons on average get deflected towards the flow axis

→ photons effectively fly a curve towards the flow axis



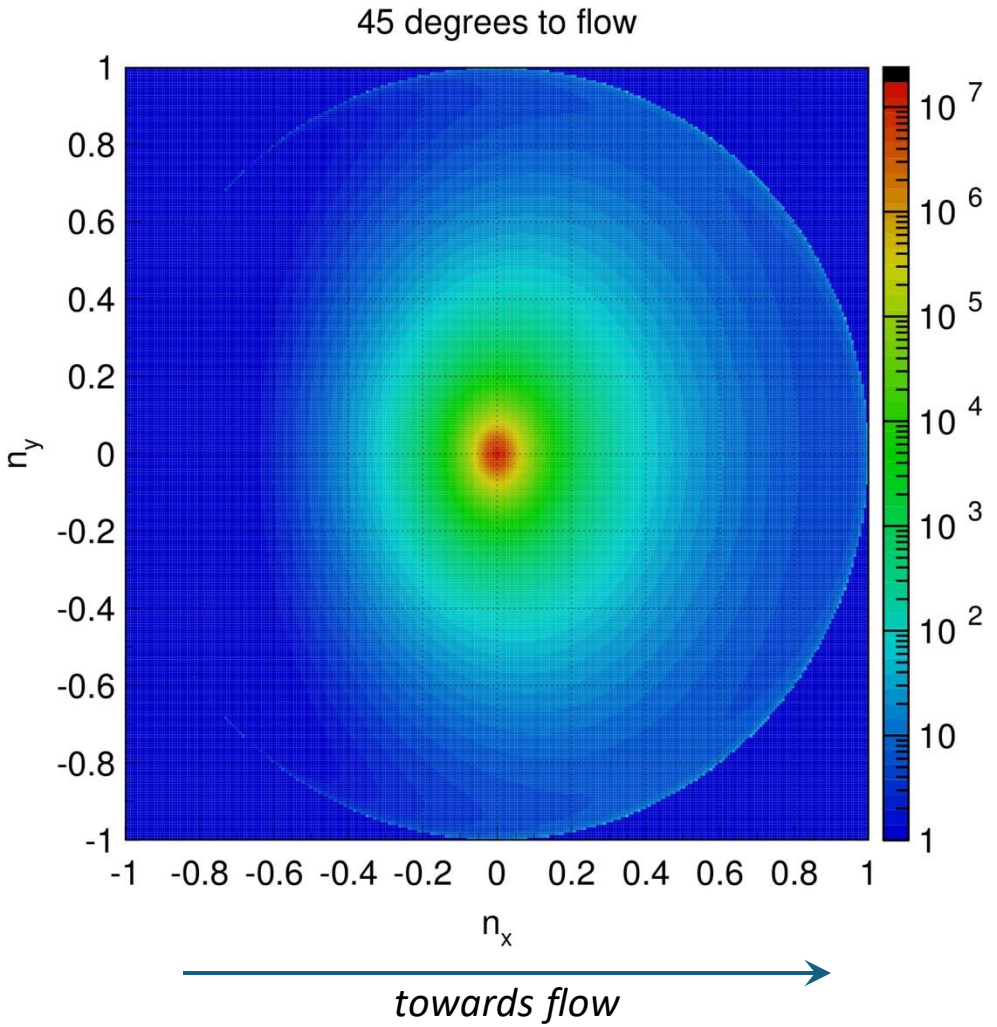




along flow

orthogonal to flow

after ~ 1 m of propagation:



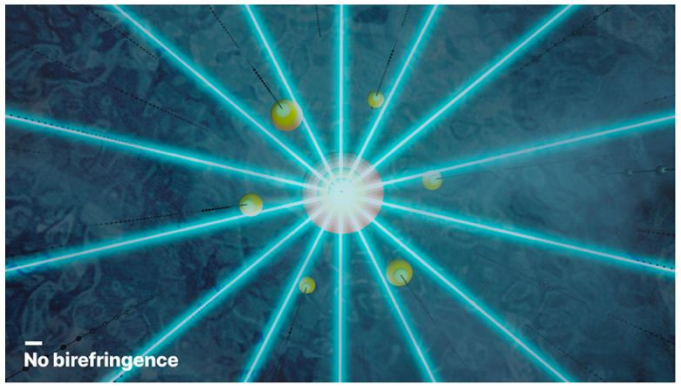
Scattering patterns birefringent ice

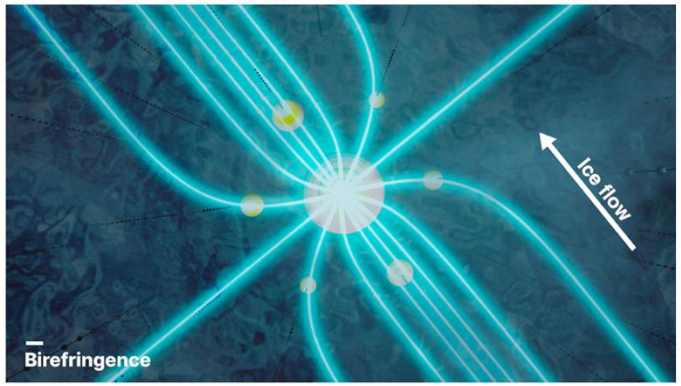
The Cryosphere, 18, 75–102, 2024
https://doi.org/10.5194/tc-18-75-2024
© Author(s) 2024. This work is distributed under
the Creative Commons Attribution 4.0 License.

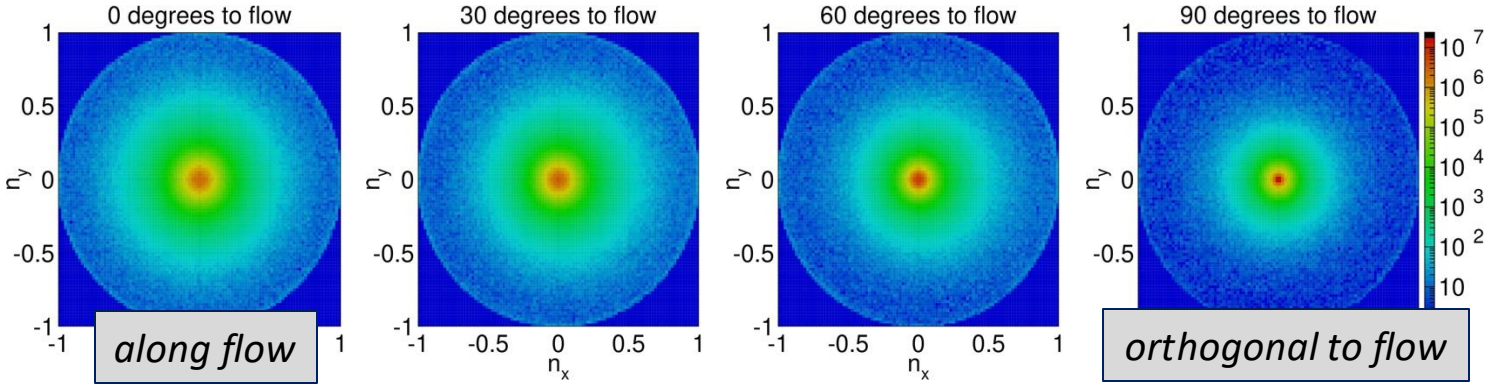
The Cryosphere Open Access EGU

2024

In situ estimation of ice crystal properties at the South Pole using LED calibration data from the IceCube Neutrino Observatory



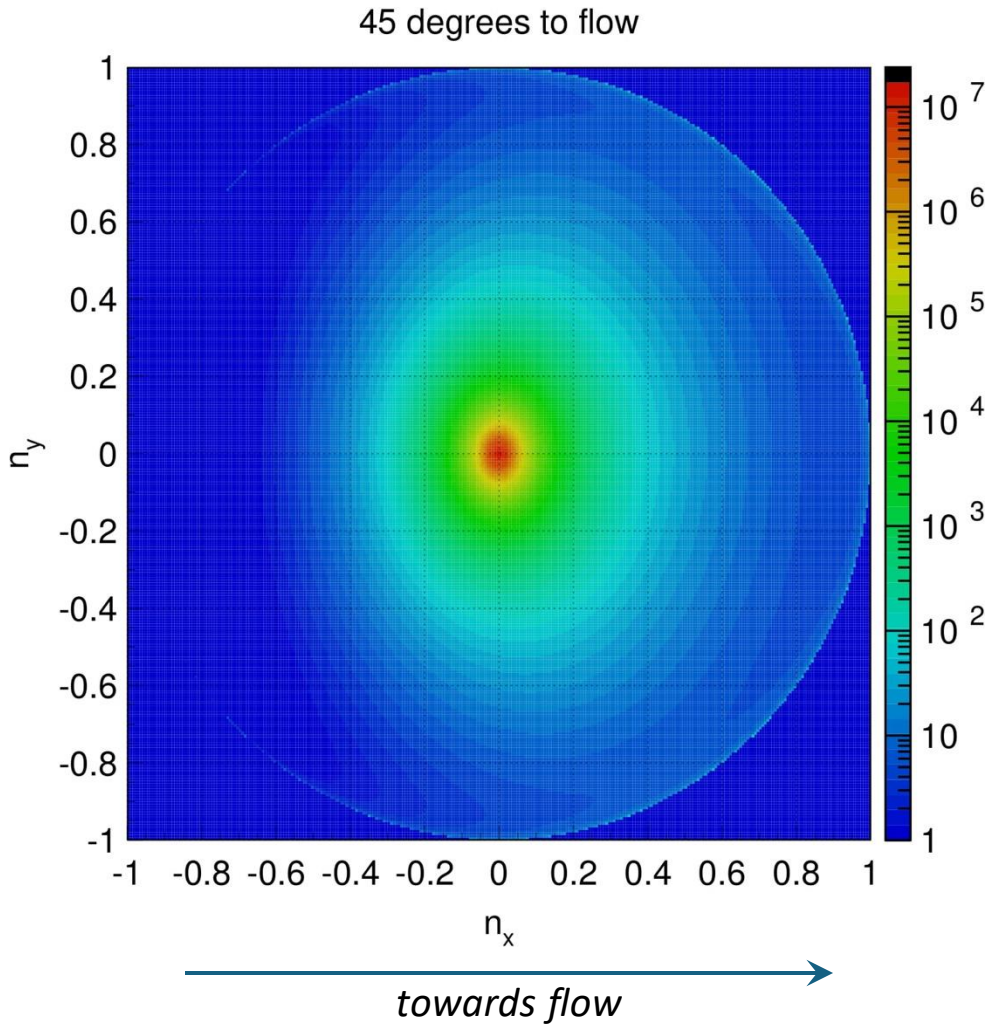




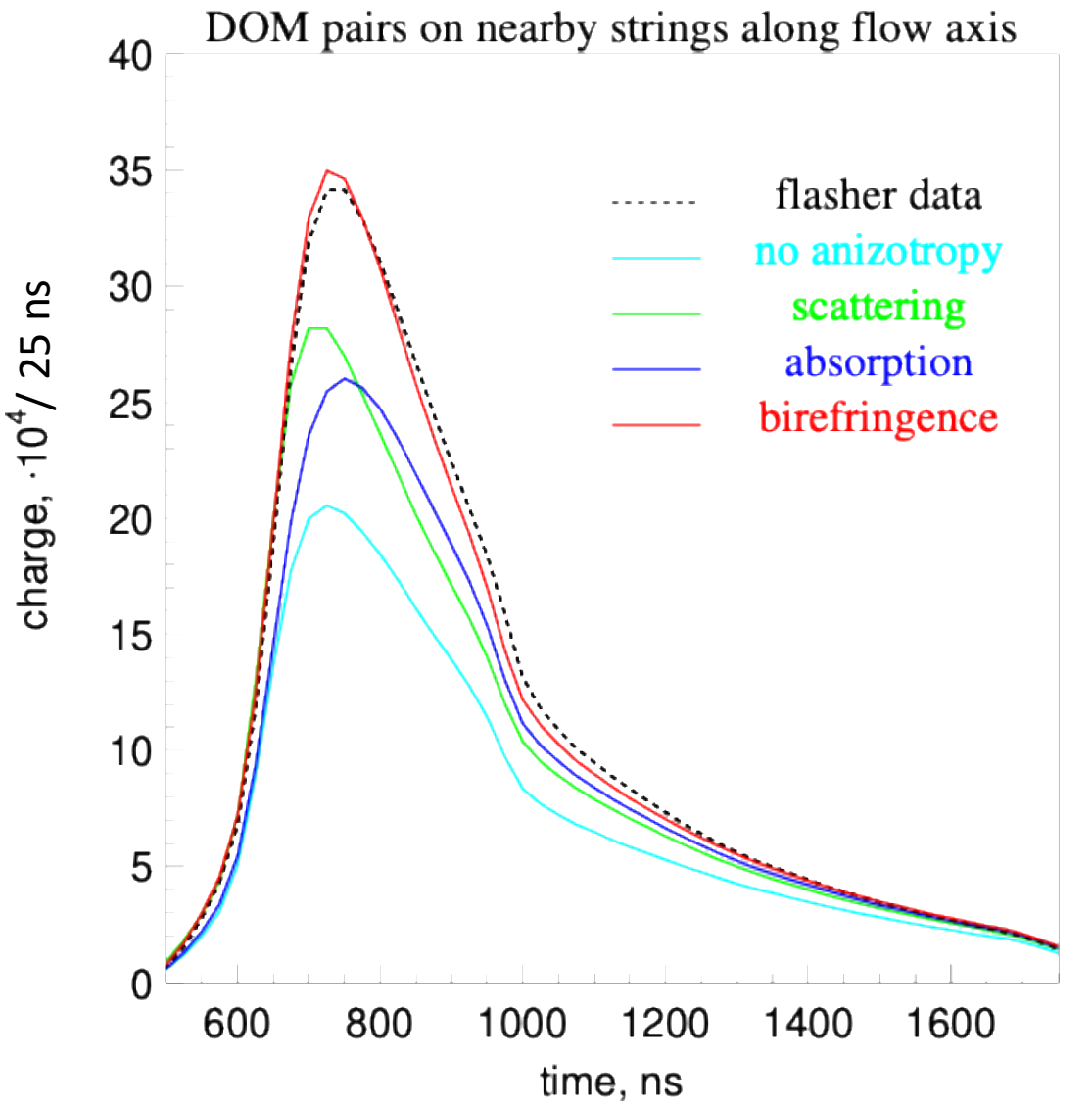
along flow

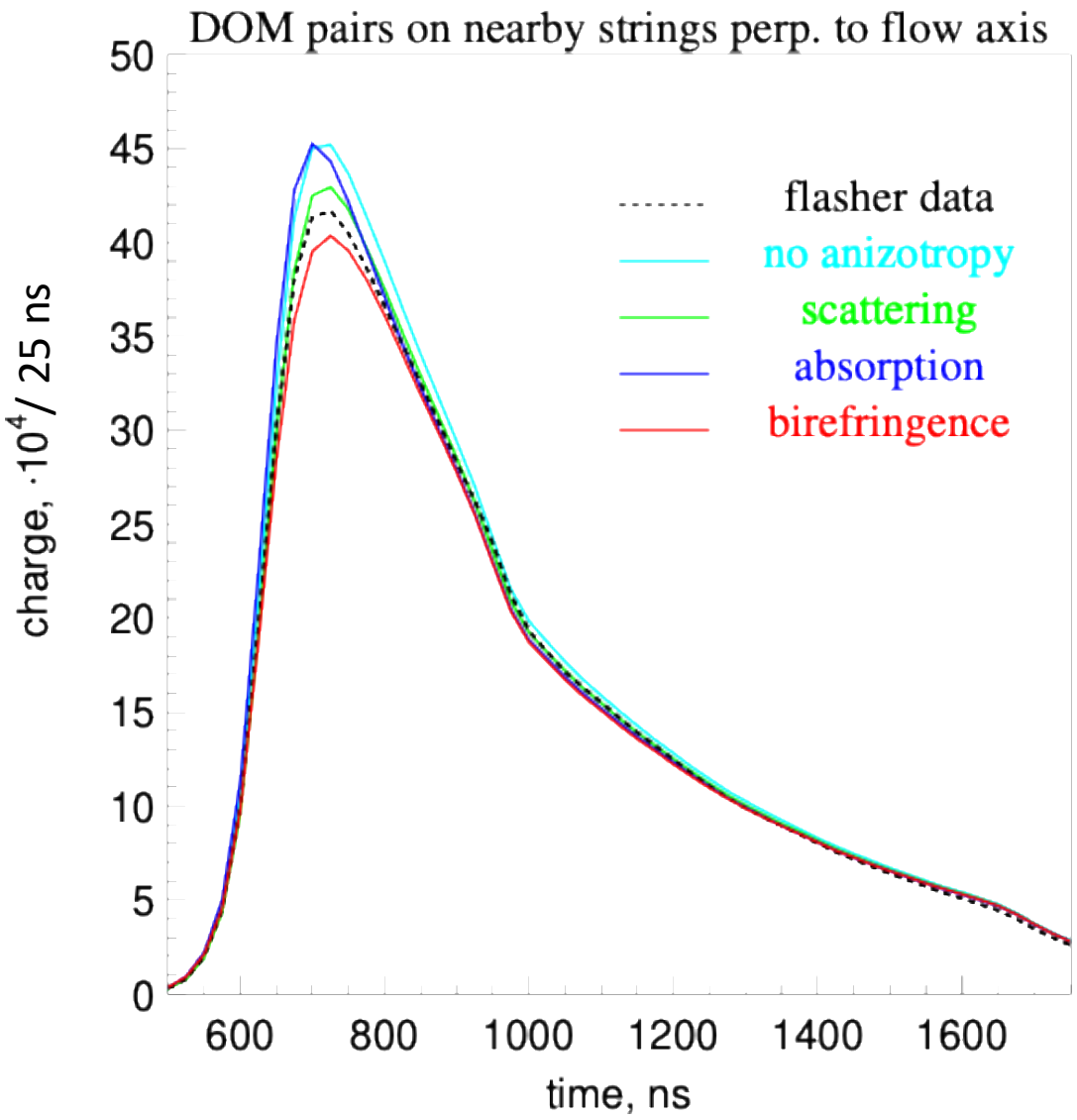
orthogonal to flow

after ~ 1 m of propagation:



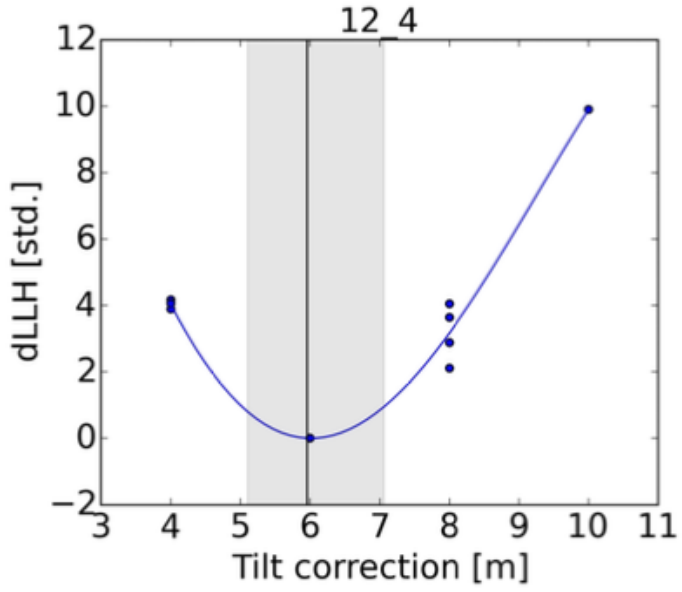
Average (at ~125 m) waveform

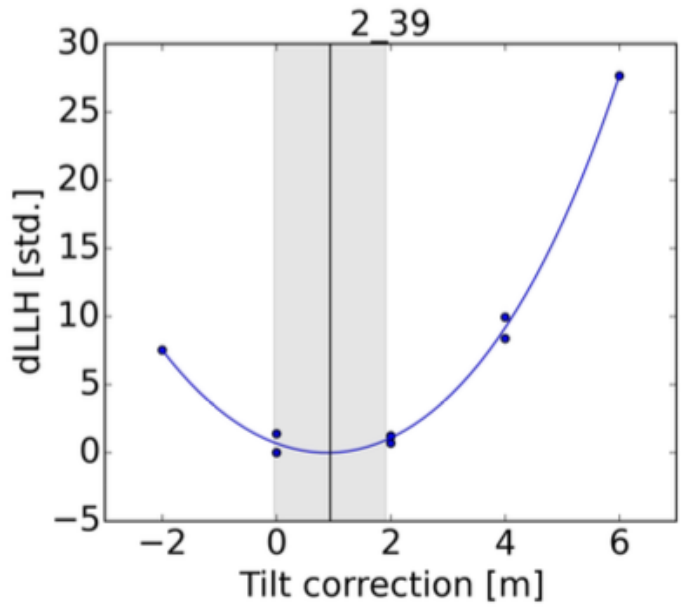


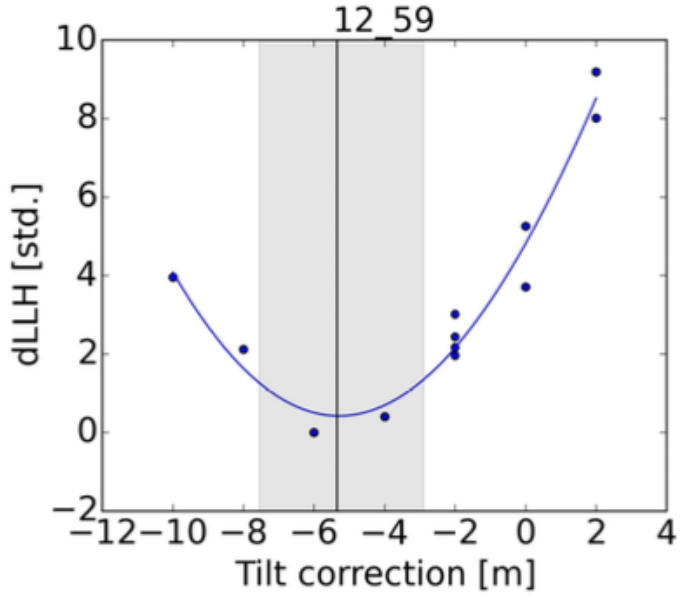


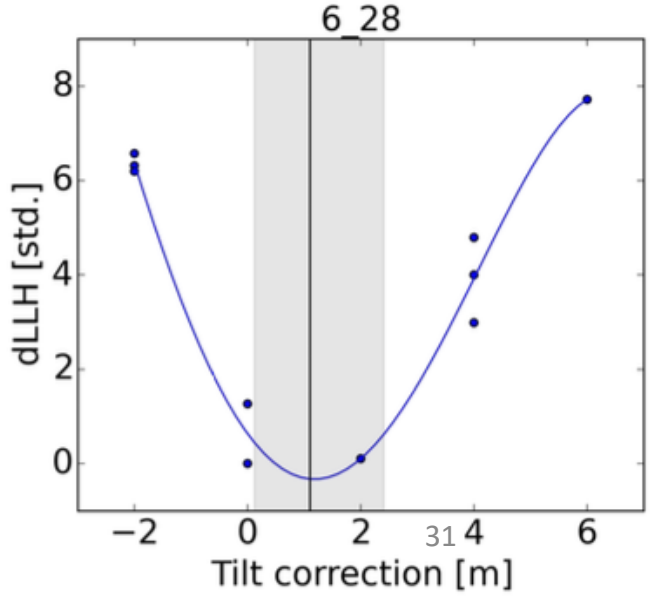
Per-DOM flasher fits

- Tilt correction in the vicinity of each DOM fitted by globally shifting the stratigraphy when optimizing its emitter flasher LLH
- Statistical uncertainty ~1m
- Extremely simple & quick fit, but with large individual biases, & methodological inconsistencies
  (reference stratigraphy no longer applicable)









Iterative Positive-Definite Fit (IPDF)

- A second-order Taylor expansion is used to fit the shape of the llh in the vicinity of best previous solution
  i.e., a paraboloid fit
  llh values are computed for nominal+100-1000 random perturbations set of simulations at each iteration

- Some regularizations are necessary
  - α: stiffness of paraboloid fit (curvature)
  - β: correlation terms (to smooth unnecessary up/down oscillations in solution)
  - γ: norm of solution (to keep it in bounds of the perturbation set)

- Search for solution (minimization)
  A direct matrix regularized inversion was tried first but often resulted in non-positive-def solutions
  Newton's gradient descent method was adopted with explicit positive-definite curvature matrix

N_{par} dimensional paraboloid describing LLH(perturbation)

Regularization terms with tunable regularization strengths α, β, γ
α: Stiffness of paraboloid; β: norm of solution; γ: smoothing correlation terms

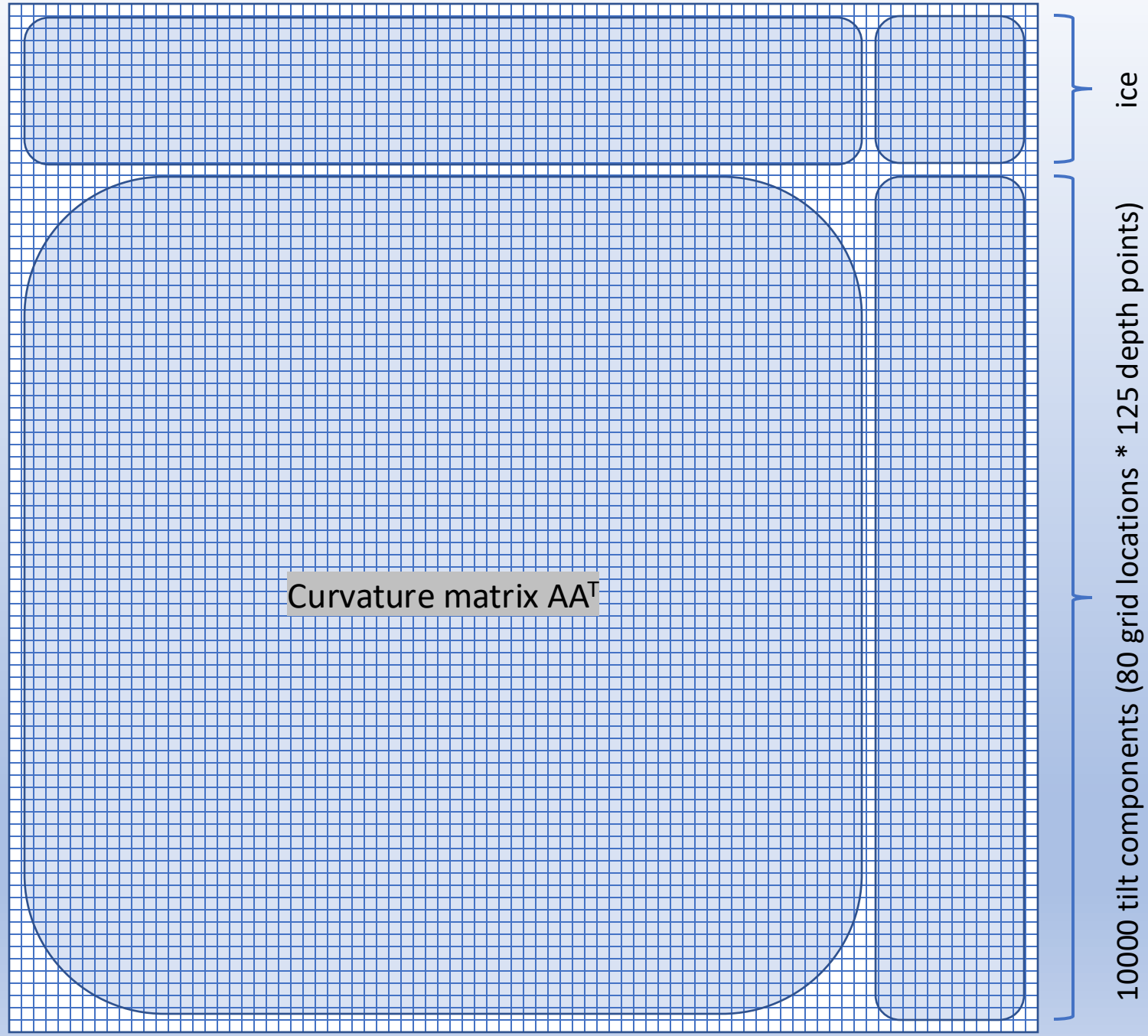
$$L = \sum_{i=1}^{N_{sim}} (Q^i + C_0 - h_i)^2 + \alpha \cdot \Big(\sum_{k,n=1}^{N_{par}} a_{kn}^2 \Big)^2 + \beta \cdot \Big(\sum_{k=1}^{N_{par}} (D_{kn}(b_n + T_n))^2 \Big)^2 + \gamma \cdot \Big(\sum_{n=1}^{N_{par}} b_n^4 \Big) \quad \text{where} \quad Q^i = \sum_{k=1}^{N_{par}} (a_{kn}(\Delta_n^i - b_n))^2$$

Value of L at the minimum

regularization term (2nd derivative, etc.)

$a_{kn}a_{km}$ is curvature matrix

deviations solution vector (main result)



Paraboloid Fit

2^{nd} order Taylor expansion around the (presumed) minimum is a paraboloid with the curvature expressed as AA^T (to enforce positive-definite quality)

Solution vector consists of:

- 10000 tilt corrections (on a grid of 80 xy locations, times 125 depth points)
- 513 ice parameters at grid point 36 (scattering, absorption, crystal density at 171 depth points)

The paraboloid is flat as possible, by regularization reducing the norm of AA^T

Additional regularizations to smooth the jaggedness in tilt solutions